BIODIVERSITY RESEARCH

WILEY | **Diversity** and **Distributions**

Projected 21st-century distribution of canopy-forming seaweeds in the Northwest Atlantic with climate change

Kristen L. Wilson[1] [iD] | Marc A. Skinner[1,2] | Heike K. Lotze[1]

[1]Department of Biology, Dalhousie University, Halifax, Nova Scotia, Canada

[2]Stantec Consulting Ltd, Dartmouth, Nova Scotia, Canada

Correspondence
Kristen L. Wilson, Department of Biology, Dalhousie University, Halifax, NS, Canada.
Email: Kristen.Wilson@dal.ca

Abstract

Aim: Climate change is predicted to alter the distribution and abundance of marine species, including canopy-forming seaweeds which provide important ecosystem functions and services. We asked whether continued warming will affect the distribution of six common canopy-forming species: mid-intertidal fucoids (*Ascophyllum nodosum*, *Fucus vesiculosus*), low-intertidal Irish moss (*Chondrus crispus*), subtidal laminarian kelps (*Saccharina latissima*, *Laminaria digitata*) and the invasive *Codium fragile*.

Location: Northwest Atlantic.

Methods: We used occurrence records and the correlative presence-only species distribution model MAXENT to determine present-day distribution. This distribution was compared to each species' warm-water physiological thresholds indicating areas of stable or reduced growth and mortality. Present-day models were then projected to mid-century (2040–2050) and end-century (2090–2100) using two contrasting carbon emission scenarios (RCP2.6 and 8.5) and two global climate models from CMIP5 based on changes in ocean temperatures.

Results: Projected range shifts were minimal under low emissions (RCP2.6), but substantial species-specific range shifts were projected under high emissions (RCP8.5), with all species except *C. fragile* predicted to experience a northward shift in their southern (warm) edge of ≤406 km by the year 2100. Northward expansions outweighed southern extirpations for fucoids and *C. crispus* leading to overall range expansions, while range contractions were projected for kelps and *C. fragile*. Model projections generally agreed with physiological thresholds but were more conservative suggesting that range shifts for kelps may be underpredicted.

Main conclusions: Our results highlight the benefits to be gained from strong climate change mitigation (RCP2.6), which would limit changes in rocky shore community distribution and composition. The business-as-usual RCP8.5 scenario projected major range shifts, seaweed community reorganization and transitions in dominant species south of Newfoundland by 2100 (~47°N). As canopy-forming seaweeds provide essential habitat, carbon storage, nutrient cycling and commercial value, understanding their response to continued climate warming is critical to inform coastal management and conservation planning.

1 | INTRODUCTION

Climate change has caused unprecedented changes in global ecosystems, resulting in species distribution shifts that alter abundance, richness and diversity patterns at different scales and across multiple taxa (e.g., Barry, Baxter, Sagarin, & Gilman, 1995; Chen, Hill, Ohlemuller, Roy, & Thomas, 2011; Hickling, Roy, Hill, Fox, & Thomas, 2006; Hiddink & ter Hofstede, 2008). As temperatures continue to increase (IPCC, 2013), major biodiversity shifts are expected (Pereira et al., 2010; Tittensor et al., 2010) as species shift to higher latitudes, altitudes or greater depth seeking cooler temperatures (Chen et al., 2011; Harley et al., 2012). Marine range shifts are more predictable (Sunday, Bates, & Dulvy, 2012) and occur at faster rates than terrestrial ones (Parmesan & Yohe, 2003; Sorte, Williams, & Carlton, 2010). Marine range shifts will affect habitat-forming species in coastal habitats, with compounding impacts on the species who depend on their ecosystem structure, functions and services (Wernberg et al., 2016; Witman & Lamb, 2018). Significant losses of habitat-forming species have already occurred in coral reefs (Carpenter et al., 2008), mangrove forests (Polidoro et al., 2010), seagrass meadows (Short et al., 2011) and seaweed beds (Krumhansl et al., 2016) due to multiple factors, and climate change poses an additional threat to many of these foundation species.

One way to examine how species may respond to climate change is with species distribution models (SDM). SDM are designed around the niche concept, where a species persists and maintains a stable population size under a given set of abiotic and biotic conditions (Hutchinson, 1957), and link known records of species presence to environmental variables (Elith et al., 2011). SDM are powerful tools to understand how species may respond to climate change, particularly if model projections can be compared to physiological data which allow for more robust projections (Elith, Kearney, & Phillips, 2010; Talluto et al., 2016). Range shift predictions based on laboratory-experiments with temperature manipulation (Piñeiro-Corbeira, Barreiro, Cremades, & Arenas, 2018) have matched observed range shifts of seaweeds in the Northeast Atlantic (NE-Atlantic) due to increasing sea surface temperature (SST; Piñeiro-Corbeira, Barreiro, & Cremades, 2016). To date, despite the widespread use of SDM for habitat-forming species (e.g., Marcelino & Verbruggen, 2015; Record, Charney, Zakaria, & Ellison, 2013; Valle et al., 2014), only two studies have incorporated the use of physiological data (Franco et al., 2018; Martínez, Arenas, Trilla, Viejo, & Carreño, 2014). The incorporation of physiological data is particularly important for invasive species which are in violation of the assumption that a species is at equilibrium with the environment (Elith et al., 2011).

Canopy-forming seaweeds are important components of coastal habitats. As ecosystem engineers (Jones, Lawton, & Shachak, 1994), they provide shelter and food to marine organisms through their complex three-dimensional structure (Schmidt, Coll, Romanuk, & Lotze, 2011). As predominant primary producers in rocky shore ecosystems (Field, Behrenfeld, Randerson, & Falkowski, 1998), they also form large quantities of biomass that store significant amounts of carbon and nutrients (Schmidt et al., 2011). These ecosystem functions and services are impacted by commercial exploitation (Seeley & Schlesinger, 2012), the spread of invasive species (Krumhansl & Scheibling, 2012; Schmidt & Scheibling, 2006, 2007), increases in turf algae (Filbee-Dexter & Wernberg, 2018), nutrient loading (Kay, Schmidt, Wilson, & Lotze, 2016; Worm & Lotze, 2006) and increasingly climate change (Filbee-Dexter, Feehan, & Scheibling, 2016; Wilson, Kay, Schmidt, & Lotze, 2015).

Sea surface temperature is the major factor influencing seaweed survival and growth on large spatial scales (Lüning, 1990), with SST isotherms closely matching seaweed distribution limits (van den Hoek, 1975). In the Northwest Atlantic (NW-Atlantic), significant surface warming has occurred since 1980 (Barnett, Pierce, & Schnur, 2001; Baumann & Doherty, 2013) resulting in northward shifts of SST isotherms (Hansen et al., 2006). This warming has important implications for canopy-forming seaweeds who dominate the rocky shores in the NW-Atlantic as local decreases in fucoid (Ugarte, Craigie, & Critchley, 2010) and kelp abundance have occurred (Dijkstra et al., 2017; Filbee-Dexter et al., 2016; Krumhansl et al., 2016). Anecdotal evidence has also suggested a small southern (warm edge) range shift for fucoids (Keser, Swenarton, & Foertch, 2005), but no large-scale shifts for kelp have been observed likely due to a lack of baseline data (Merzouk & Johnson, 2011). Elsewhere, range shifts of seaweeds have been observed in Portugal (Lima, Ribeiro, Queiroz, Hawkins, & Santos, 2007), Spain (Duarte et al., 2013), Britain (Gallon et al., 2014; Yesson, Bush, Davies, Maggs, & Brodie, 2015), Australia (Wernberg et al., 2011, 2016) and Japan (Tanaka, Taino, Haraguchi, Prendergast, & Hiraoka, 2012), and these shifts have been attributed to climate change. As the projected warming trends continue over the 21st century (IPCC, 2013), large-scale distribution shifts of seaweed communities in the NW-Atlantic are expected (Assis, Araújo, & Serrão, 2018a; Assis, Serrão, Claro, Perrin, & Pearson, 2014; Jueterbock et al., 2013; Müller, Laepple, Bartsch, & Wiencke, 2009).

This paper assessed how projected scenarios of future climate change will impact the distribution of common native and invasive canopy-forming seaweeds in the NW-Atlantic spanning intertidal and subtidal habitats. Our objectives were to: (a) create a database of occurrence records to determine present-day range limits; (b) use these occurrence records to build SDM to predict current and

project future distributions under different climate-change scenarios; and (c) compare the SDM to physiological thresholds to assess the accuracy of projections and identify areas of stable growth versus reduced growth and/or mortality. We hypothesized species-specific northward range shifts, which would alter the composition of canopy-forming seaweeds along the NW-Atlantic coast. Any range shifts would have important consequences for ecosystem structure, functions and services, with implications for management and conservation.

2 | METHODS

2.1 | Seaweed flora of the NW-Atlantic

We focused on six representative species with different zonation patterns across NW-Atlantic rocky shores: mid-intertidal fucoids (*Ascophyllum nodosum*, *Fucus vesiculosus*), low-intertidal Irish moss (*Chondrus crispus*), subtidal laminarian kelps (*Laminaria digitata*, *Saccharina latissima*) and the invasive *Codium fragile*. Originating from Japan (Provan, Booth, Todd, Beatty, & Maggs, 2008), *C. fragile* was first introduced to the NW-Atlantic in Long Island Sound in 1957 (Carlton & Scanlon, 1985) and competes with native kelp species (Scheibling & Gagnon, 2006).

In the NW-Atlantic, *A. nodosum*, *C. crispus* and kelps exist south to Long Island Sound and *F. vesiculosus* and *C. fragile* south to North Carolina (Adey & Hayek, 2011; Carlton & Scanlon, 1985; Lüning, 1990; Taylor, 1957). Each species exhibits a continual distribution from their southern (warm edge) limit to southern Labrador for *C. crispus* and *C. fragile* (Adey & Hayek, 2011; Matheson, Mckenzie, Sargent, Hurley, & Wells, 2014) and north to the Hudson Strait for the other four species. Kelps and *F. vesiculosus* occur in Hudson Bay (Mathieson, Moore, & Short, 2010; McDevit & Saunders, 2010), fucoids and *S. latissima* in Western Greenland (Høgslund, Sejr, Wiktor, Blicher, & Wegeberg, 2014; Marbà et al., 2017), and *F. vesiculosus* and *S. latissima* into the high Arctic (Filbee-Dexter, Wernberg, Fredriksen, Norderhaug, & Pedersen, 2019).

We collected presence-only occurrence records from the literature and regional experts (Supporting Information Tables S1.1–S1.6 in Appendix S1) to determine each species present-day distribution. Generally, records were collected from 1980 onwards, as this was the first year significant increases in SST were detected in the NW-Atlantic (Barnett et al., 2001). However, few occurrence records exist for the Arctic due to their inaccessibility. Therefore, additional records prior to 1980 were used north of Newfoundland (47°N), where seaweeds that were present prior to 1980 could still occur after 1980 as any Arctic warming would promote northward range shifts. As the environmental layers do not perfectly match the coastline, occurrence records that did not overlay the environmental data were moved to the closest pixel. All records were projected into the Behrmann cylindrical equal-area projection (see following section) using ArcGIS® 10.5 (ESRI, 2011), and duplicate records within a pixel were removed.

2.2 | Environmental data

The global marine environmental dataset Bio-Oracle 2.0 was used to represent present-day conditions which provide long-term averages (LTA) from 2000 to 2014, in Behrmann cylindrical equal-area projection, at a 7 km pixel resolution (Assis, Tyberghein et al., 2018b; Tyberghein et al., 2012). All pixels >100 km from shore were excluded from analysis and environmental data were cropped from 32–84°N and 42–95°W within the statistical environment R (R Core Team, 2014) using the "sdmpredictors" package (Bosch, Tyberghein, & De Clerck, 2018). To incorporate the range of environmental conditions seaweeds encounter during the year, we incorporated LTA of the maximum (e.g., warmest) month (*M*-max) and the minimum (e.g., coolest) month (*M*-min) for SST, sea surface salinity (SSS), sea ice coverage (SIC), current velocity (CV) and sea surface nitrate (NO_3^-) for the three intertidal species (fucoids, *C. crispus*) as well as yearly LTA minimum and maximum (*Y*-max, *Y*-min) diffuse attenuation (DA) for the subtidal species (kelps, *C. fragile*), all of which are known to impact seaweed growth and survival (Harley et al., 2012). All environmental data layers were retained based on a Pearson's correlation coefficient ≤0.90 and variable inflation factor ≤10 (Naimi & Araújo, 2016).

To project onto future climate, we choose two global climate models from CMIP5 (Taylor, Stouffer, & Meehl, 2012), one projecting lower (GFDL-ESM2M; GFDL hereafter; Dunne et al., 2012) and one higher (IPSL-CM5A-LR; IPSL hereafter; Dufresne et al., 2013) levels of SST warming (Bopp et al., 2013). In addition, we used two representative concentration pathways (RCP): a low carbon emission and strong mitigation scenario (RCP2.6) and a high emission business-as-usual scenario (RCP8.5; Moss et al., 2010). This combination of two climate models and two RCPs provides a range of best- to worst-case scenarios of warming over the next century (Bopp et al., 2013). LTAs of SST *M*-max and *M*-min were derived for present-day (2006–2015), mid-century (2040–2050) and end-century (2090–2100) for each climate model and RCP scenario. Present-day was chosen to begin in 2006 as this was the year CMIP5 climate models switch from historical runs to future projections forced by each RCP scenario. To account for the differences between present-day observed (from Bio-Oracle) and projected (from GFDL and IPSL) environmental data, we calculated relative changes in SST *M*-max and *M*-min for future periods (mid-century minus present-day; end-century minus present-day) for each climate model and RCP scenario. This relative change (anomaly) in SST was then added to the present-day observed SST. All projections are based on ocean temperature and the climate model data were re-gridded to the 7 km grid used for present-day environmental layers.

2.3 | SDM building, evaluation and projection

The correlative SDM was built using Maxent 3.3.3k (Phillips, Anderson, & Schapire, 2006; Phillips, Dudík, & Schapire, 2004) within R using the "dismo" package (Hijmans, Phillips, Leathwick, & Elith, 2017). Maxent consistently performs well compared to other

TABLE 1 Climate variables included in the variable selection process with their percent contribution (PC; %), permutation importance (PI; %), average training and test gain and AUC, and the value for maximizing the sum of test sensitivity and specificity (MTSS) logistic threshold (LT; bolded value indicates binomial probability of $p < 0.001$) for the cross-validation runs ($k = 5$) and full run ($k = 1$) indicating the order of variable removal (OR; bolded variables included in best model). See methods and Supporting Information Table S2.3 for variable long names

		A. nodosum			F. vesiculosus			C. crispus			C. fragile			L. digitata			S. latissima		
		OR	k=5	k=1	OR	k=5	k=1	OR	k=5	k=1	OR	k=5	k=1	OR	k=5	k=1	OR	k=5	k=1
PC	SST M-max	8	10.49	10.22	10	22.45	20.97	7	14.45	12.26	10	24.30	27.74	11	21.43	21.29	11	7.50	10.57
	SST M-min	10	35.49	37.06	5			10	51.94	52.91	6			6			2		
	SSS M-max	3	6.73	6.62	7	7.24	9.53	8	18.57	20.13	4			8	7.34	7.11	5	7.50	5.65
	SSS M-min	5			1			5			3			3			1		
	SIC M-max	7	20.21	20.12	8	47.71	47.84	2			12	28.61	25.93	10	27.33	28.42	9	29.84	27.14
	SIC M-min	2			3			4			5			4			7	0.66	0.86
	NO₃⁻ M-max	4	3.02	3.60	2			1			2			1			3		
	NO₃⁻ M-min	9	18.60	18.33	9	22.60	21.67	9	15.05	14.70	1			9	10.22	9.61	10	11.23	11.14
	CV M-max	1			4			3			8	3.60	3.56	2			6	0.70	0.74
	CV M-min	6	5.47	4.04	6			6			7			5			4		
	DA Y-max	N/A			N/A			N/A			9	34.69	34.14	12	33.68	33.57	12	36.95	38.68
	DA Y-min	N/A			N/A			N/A			11	8.79	8.63	7			8	5.62	5.22
PI	SST M-max	8	6.69	7.32	10	18.04	16.34	7	7.69	8.77	10	57.33	55.96	11	9.19	11.40	11	10.05	18.41
	SST M-min	10	43.05	50.31	5			10	61.27	61.46	6			6			2		
	SSS M-max	3	9.80	7.90	7	9.00	7.69	8	20.56	20.57	4			8	20.98	20.86	5	5.47	7.24
	SSS M-min	5			1			5			3			3			1		
	SIC M-max	7	13.67	12.33	8	54.96	57.99	2			12	12.63	12.91	10	43.91	46.82	9	44.39	34.77
	SIC M-min	2			3			4			5			4			7	2.13	2.58
	NO₃⁻ M-max	4	3.30	3.31	2			1			2			1			3		
	NO₃⁻ M-min	9	18.32	15.64	9	18.00	17.98	9	10.48	9.20	1			9	9.86	6.24	10	17.33	13.89
	CV M-max	1			4			3			8	8.50	9.03	2			6	2.67	5.73
	CV M-min	6	5.17	3.18	6			6			7			5			4		
	DA Y-max	N/A			N/A			N/A			9	11.04	12.68	12	16.06	14.68	12	9.77	8.31
	DA Y-min	N/A			N/A			N/A			11	10.51	9.42	7			8	8.20	9.08
	Training Gain		1.87	1.78		1.46	1.46		2.09	2.08		2.80	2.78		2.16	2.12		1.79	1.78
	Training AUC		0.96	0.95		0.92	0.92		0.96	0.96		0.98	0.98		0.96	0.96		0.94	0.94
	Test Gain		2.01	N/A		1.51	N/A		2.11	N/A		2.92	N/A		2.16	N/A		1.79	N/A
	Test AUC		0.95	N/A		0.91	N/A		0.96	N/A		0.98	N/A		0.95	N/A		0.92	N/A
	MTSS LT		**0.20**	N/A		**0.30**	N/A		**0.17**	N/A		**0.14**	N/A		**0.15**	N/A		**0.23**	N/A

correlative presence-only modelling algorithms (Elith et al., 2006). Each species present-day distribution was built using *k*-fold cross-validation with *k* = 5 (Kohavi, 1995), allowing for linear, quadratic and hinge feature classes (Elith et al., 2011; Phillips et al., 2006), and set to 5,000 iterations. Continuous model output was turned into binary presence/absence data based on maximizing the sum of test sensitivity and specificity threshold (Liu, Newell, & White, 2016). Model performance was evaluated using a one-tailed binomial test, and with the area under the curve (AUC) of the receiver operator characteristics curve (Phillips et al., 2006). A jackknife test as implemented by MAXENT was performed to determine the importance of each environmental variable, and the variable with the smallest decrease in average test gain when removed from the full model was dropped. This was repeated until only one variable remained to determine the most important variable for predicting each species' distribution. To balance variables that performed well in training and testing, average regularized training gain was used to determine the best model for each species. This balanced model complexity and performance, where the best model was determined to have the fewest number of predictor variables that did not result in a significantly different training gain from the full model, based on 95% confidence intervals (Yost, Petersen, Gregg, & Miller, 2008). Therefore, test gain was used to decide which variables to remove, while training gain was used to decide when to stop removing variables.

Once the best SDM was determined per species, each species' SDM was rerun using the full set of occurrence records to ensure the models were trained under the full set of environmental conditions they may experience (*k* = 1). This was repeated for present-day observed conditions, and relative projected mid-century and end-century conditions for both climate models and RCP scenarios. The future projections used present-day environmental conditions for all variables but switching the SST terms for the climate data calculated above. We projected with SST terms for all six species as SST *M*-max was retained as an important climatic driver within the best model per species, contributing at least 5% to the models, and warming ocean temperatures are a major driver of climate change. Two species were also projected with SST *M*-min as this was also retained in their best models (see below). Models were clamped to avoid training with data outside the species range (Elith et al., 2010).

2.4 | Physiological thresholds

A previous laboratory experiment (Wilson et al., 2015) provided information on the growth and survival of all study species except *S. latissima* between 12 and 29°C from populations found in the middle of each species respective range in Atlantic Canada. *Saccharina latissima* was assumed to experience similar growth as *L. digitata* based on experimental studies completed on *S. latissima* populations from Halifax (Bolton & Lüning, 1982; Simonson, Scheibling, & Metaxas, 2015), Maine, and Long Island Sound (Redmond, 2013). These data were used to create three physiological thresholds (PTs) for heat-related growth and survival to define the water temperatures at which each species experienced reduced growth, reduced

growth and partial mortality, and complete mortality. Reduced growth was defined as the first temperature at which there was a statistically significant growth rate reduction, partial mortality was at least one replicate dying, and complete mortality was all replicates dying at a specific temperature. See Supporting Information Table S2.1 and Figure S2.1 in Appendix S2 for the data supporting our PT. Cold-related survival was not tested but all species exhibit measurable photosynthesis in water temperatures of at least 0°C (Lüning, 1990). Present-day and projected future SST *M*-max data were classified into these three categories, creating a layer for each species' PT (Martínez et al., 2014).

We compared our PTs to the results of the SDM which allowed us to confirm the accuracy of projected range shifts based on SST changes (Franco et al., 2018; Martínez et al., 2014). To do so, the predicted present-day and projected future SDM were overlaid onto the corresponding species' PT. Areas corresponding to PTs for stable and reduced growth were likely to contain suitable habitat, while areas corresponding to PTs for reduced growth and partial mortality, or complete mortality were less likely to contain suitable habitat and may indicate areas with greater susceptibility to multiple stressors in a warming climate. In the following written section, we classify all areas that do not indicate stable growth as "poor growth" for simplicity. The reader is directed to Table 2 and the associated figure per species for the exact PT category and associated temperature. Seaweed thermal performance curves are useful tools to predict the response to projected warming scenarios (Harley et al., 2012), and our PTs were used to reflect growth optima and important inflection points. We displayed SSTs in 1°C increments to account for the possibility that an inflection point occurred within the 3°C temperature range for each PT, and for the possible acclimation to different SST across a species range.

3 | RESULTS

3.1 | Variable importance

We considered 12 environmental variables to be included in the variable selection process for the subtidal species, and 10 for the intertidal species (Supporting Information Tables S2.2 and S2.3 in Appendix S2). Each variable was removed in a backward selection process based on the jackknife test implemented by MAXENT (Table 1). Variables with the smallest decrease in test gain were removed until there was a significant decrease in training gain based on 95% confidence intervals (Supporting Information Figures S2.2 and S2.3). The suggested variable to remove based on test gain was typically the same as the variables based on training gain and AUC. Furthermore, 95% confidence intervals based on training AUC also typically suggested the best model as those suggested by training gain, corroborating the robustness of the resulting best models.

Mean SST of the warmest month on average (*M*-max) was the only variable retained in the best model for all six species, yearly maximum diffuse attenuation (DA *Y*-max) for all subtidal species and mean sea ice coverage of the month with highest coverage on average (SIC *M*-max)
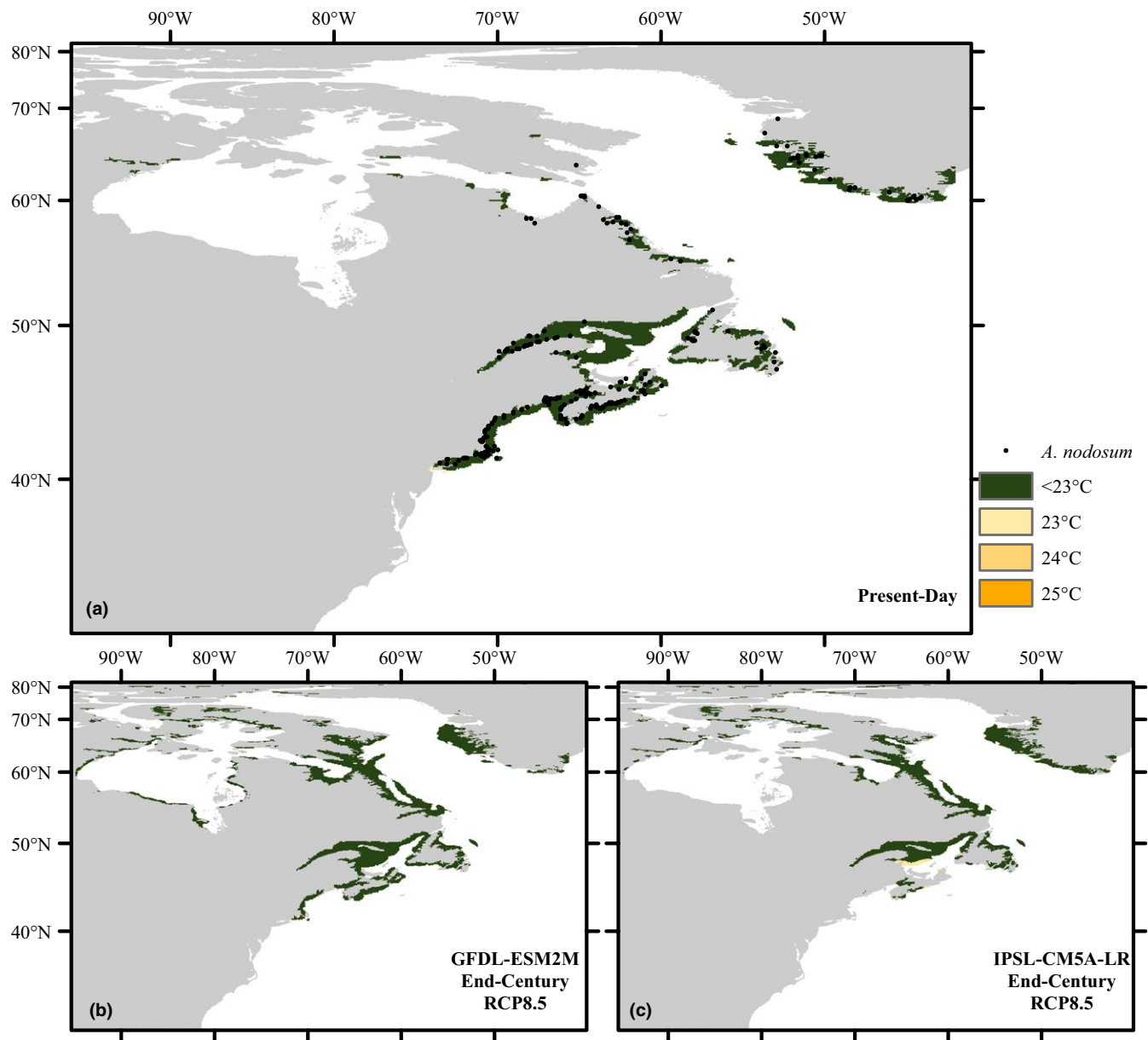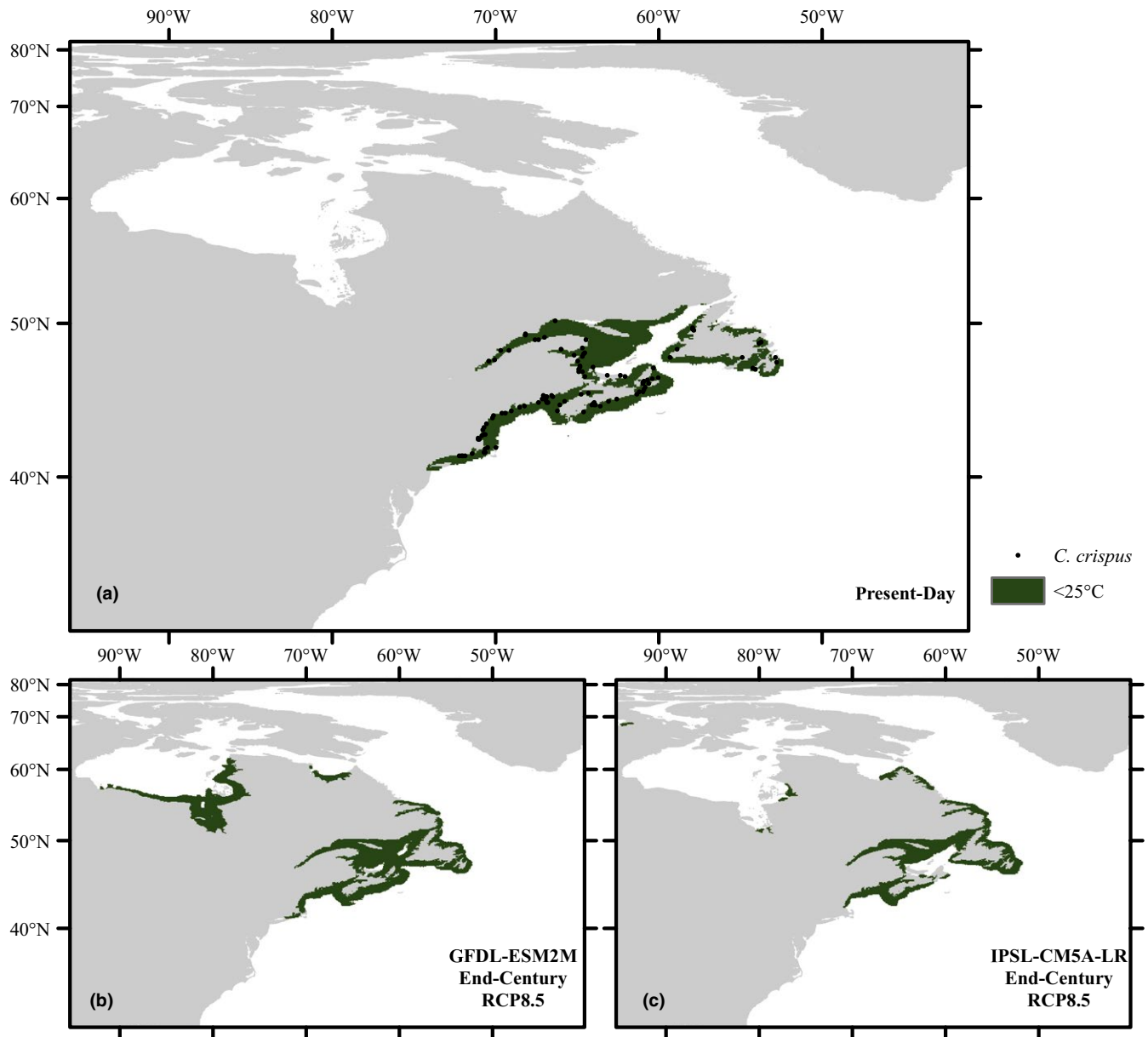
FIGURE 1 Distribution of *Ascophyllum nodosum*: (a) present-day occurrence records (black dots) and SDM, and projected (b, c) end-century distribution based on SST changes under RCP8.5 from GFDL-ESM2M (left column) and IPSL-CM5A-LR (right column; Behrmann world equal-area projection). Physiological thresholds were overlaid to show areas of stable growth (green, 12–22°C) and reduced growth (yellow-orange, 23–25°C); no areas of reduced growth and partial mortality (pink-red, 26–28°C) or complete mortality (dark red, ≥29°C) were observed. Pixels that appear to be on land are in narrow fjords

for five species (Table 1). Only *A. nodosum* and *C. crispus* retained mean SST of the coolest month on average (*M*-min). Based on permutation importance, SST *M*-min was the most important climatic variable for *A. nodosum* and *C. crispus*, SIC *M*-max for *F. vesiculosus*, *L. digitata* and *S. latissima*, and SST *M*-max for *C. fragile*. All models had a significant binomial *p*-value and an AUC >0.90, indicating high model performance.

3.2 | Present-day distributions

Presently, *A. nodosum* (Figure 1a), *C. crispus* (Figure 2a), *L. digitata* (Figure 3a) and *S. latissima* (Figure 4a) were correctly predicted to

occur south to ~40°N (Table 2; Adey & Hayek, 2011; Carlton & Scanlon, 1985; Lüning, 1990; Taylor, 1957). *Fucus vesiculosus* occurred further south to ~36°N, but the southern range limit likely extends further southward based on occurrence records (Figure 5a). *Codium fragile* is not known to extend southward to the predicted southern (warm edge) range limit of ~32°N (Figure 6a). The occurrence records used to train the SDM aligned well with the PTs, with no records occurring at SST *M*-max values indicating complete mortality (Figure 7). Furthermore, the allocation of the predicted area to SST *M*-max for poor growth was <3% for fucoids and *C. crispus*, <7% for the kelps, and ~12% for *C. fragile* (Table 2).
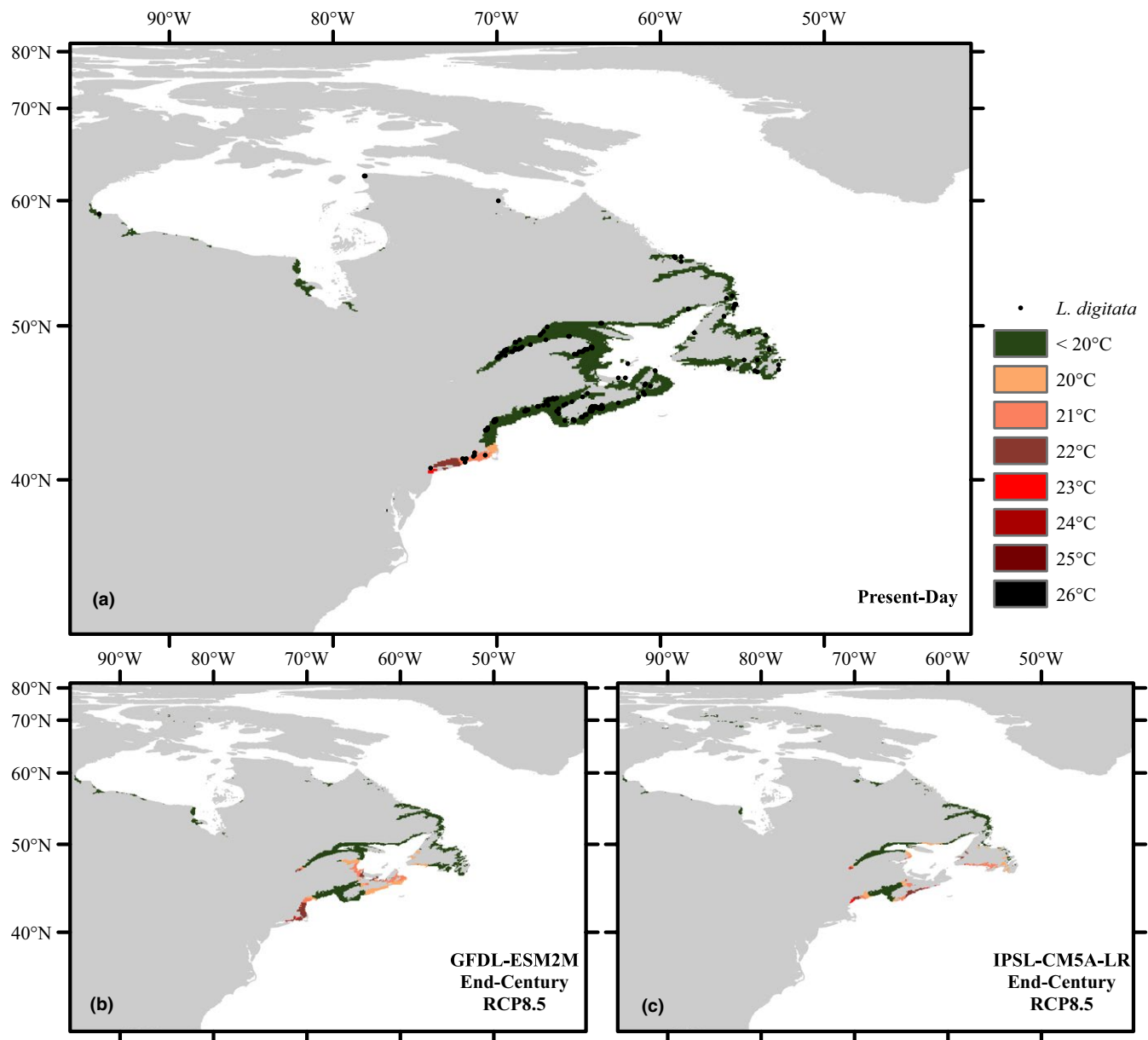
FIGURE 2 Distribution of *Chondrus crispus*: (a) present-day occurrence records (black dots) and SDM, and projected (b, c) end-century distribution based on SST changes under RCP8.5 from GFDL-ESM2M (left column) and IPSL-CM5A-LR (right column; Behrmann world equal-area projection). Physiological thresholds were overlaid to show areas of stable growth (green, 12–28°C); no areas of reduced growth (yellow-orange, ≥29°C) were observed. Pixels that appear to be on land are in narrow fjords

The northern distribution limit of *A. nodosum* extends along the Labrador coast to ~67°N (Figure 1a). *Chondrus crispus* (Figure 2a) and *C. fragile* (Figure 6a) occur north to ~51°N in southern Labrador, and the predicted habitat areas aligned well with known occurrence records. *Laminaria digitata*'s northern range was slightly underpredicted in western Hudson Bay, but based on occurrence records, its northern limit is ~62°N (Figure 3a). The northern range limits of *F. vesiculosus* (Figure 5a) and *S. latissima* (Figure 4a) were difficult to quantify as their northern distributions were underpredicted, but occurrence records suggest they occur to ~71°N and ~77°N, respectively. The combined present-day distributions of all species show maximum richness of

canopy-forming seaweeds from Long Island Sound to southern Labrador (Figure 8a).

3.3 | Seaweed flora under a strong mitigation scenario (RCP2.6)

Sea surface temperature *M*-max (mean SST of the warmest month on average) was retained in the best models by all six species, was in the top four variables based on test gain and contributed >5% to permutation importance and percent contribution (Table 1). SST *M*-min was retained by two species and was the most important environmental variable for *A. nodosum* and *C. crispus*. Therefore, future projections

FIGURE 3 Distribution of *Laminaria digitata*: (a) present-day occurrence records (black dots) and SDM, and projected (b, c) end-century distribution based on SST changes under RCP8.5 from GFDL-ESM2M (left column) and IPSL-CM5A-LR (right column; Behrmann world equal-area projection). Physiological thresholds were overlaid to show areas of stable growth (green, 12–19°C), reduced growth and partial mortality (pink-red, 20–22°C), and complete mortality (dark red, ≥23°C). Pixels that appear to be on land are in narrow fjords

for all species were based on present-day conditions for the other environmental variables while changing the SST M-max values for all species and the SST M-min terms for *A. nodosum* and *C. crispus*.

By end-century, following strong carbon mitigation under the RCP2.6 scenario, changes of the southern (warm) distribution edge were limited to a maximum of 40 km (0.4°) shift north for all species based on the average response of the mild (GFDL) and strong (IPSL) warming models by 2100 (Table 2). A larger poleward range shift was projected by 2050, yet some equatorial range expansion from 2050 to 2100, cumulated into a small poleward range shift that persisted to 2100. These range shifts corresponded to a decrease of areas

with poor growth based on the PTs for *F. vesiculosus* and *C. fragile*, no change for *C. crispus*, but increases for *A. nodosum* and kelps.

Northern range expansions were projected for *A. nodosum* (Supporting Information Figure S2.4) leading to an average increase of 30% (118,605 km^2) of total habitat area by 2100 (Table 2). Note that all area measurements indicate a maximum value as not all area within a pixel may contain suitable habitat. Smaller northern expansions were projected for *F. vesiculosus* (Supporting Information Figure S2.5), *C. crispus* (Supporting Information Figure S2.6), and *C. fragile* (Supporting Information Figure S2.7) leading to an average increase of total habitat area by 1%, 16% and 6% by 2100, respectively
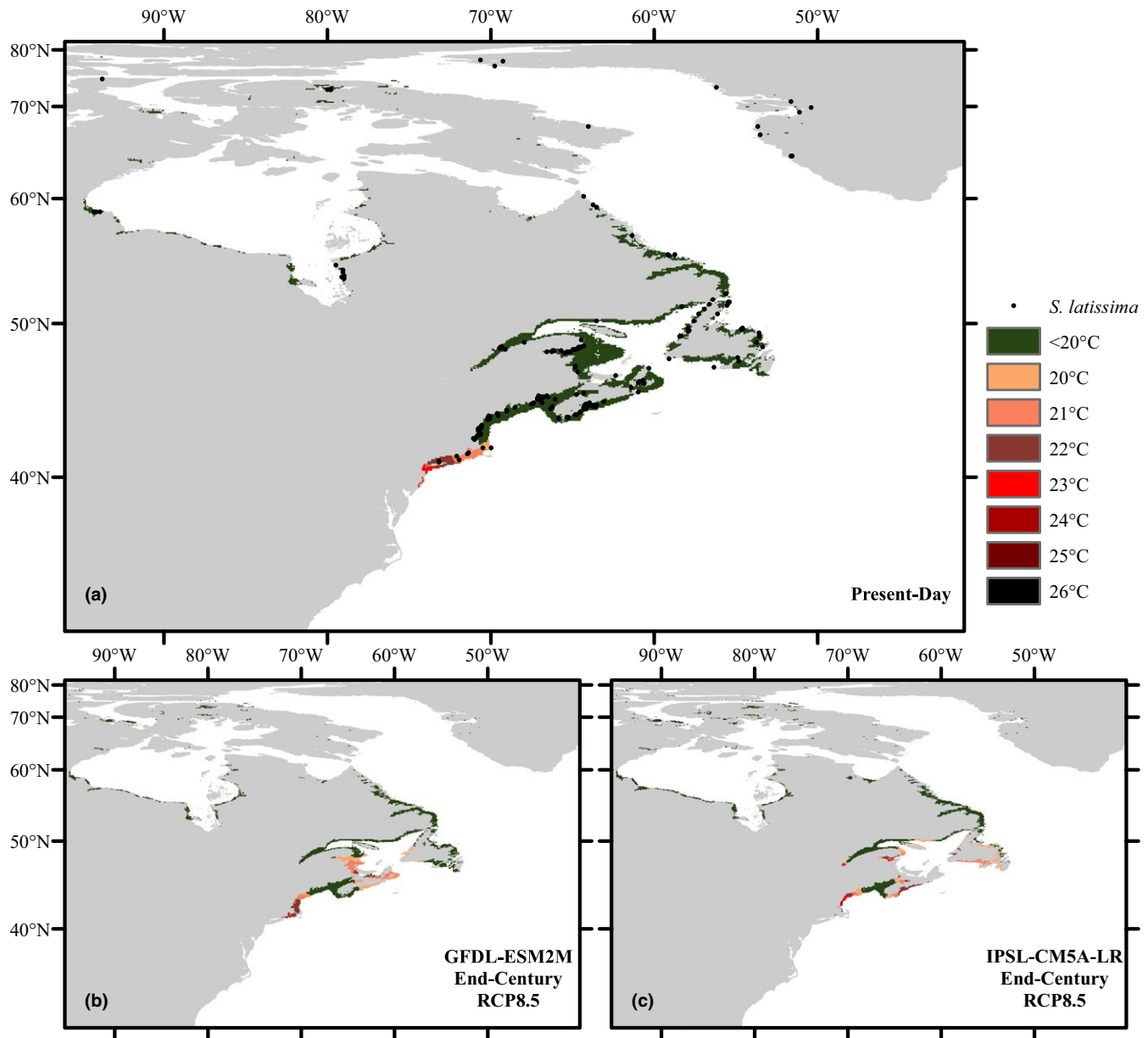
FIGURE 4 Distribution of *Saccharina latissima*: (a) present-day occurrence records (black dots) and SDM, and projected (b, c) end-century distribution based on SST changes under RCP8.5 from GFDL-ESM2M (left column) and IPSL-CM5A-LR (right column; Behrmann world equal-area projection). Physiological thresholds were overlaid to show areas of stable growth (green, 12–19°C), reduced growth and partial mortality (pink-red, 20–22°C), and complete mortality (dark red, ≥23°C). Pixels that appear to be on land are in narrow fjords

(Table 2). *Laminaria digitata* (Supporting Information Figure S2.8) was projected to lose 4% of its average total habitat area while *S. latissima* (Supporting Information Figure S2.9) showed little change (Table 2). Furthermore, no changes in seaweed species richness were projected under RCP2.6 (Supporting Information Figure S2.10).

3.4 | Seaweed flora under a business-as-usual scenario (RCP8.5)

By end-century, northward shifts of the southern (warm) range limits were projected for all species except for *C. fragile* (Table 2). Unlike RCP2.6, these range shifts begin by 2050 and continue through to 2100 (Figures 1–6; Supporting Information Figures S2.4–S2.9). Note that the projected range shift values indicate the magnitude of the shift towards the poles, the length of range shift along the coastline would be greater.

By 2100, the southern distribution limits for *A. nodosum* (Figure 1b,c), *L. digitata* (Figure 3b,c) and *S. latissima* (Figure 4b,c) were projected to shift to the Gulf of Maine or Bay of Fundy, depending on the climate model, with additional decreases in habitat suitability along the Atlantic coast of Nova Scotia and Gulf of St. Lawrence. The Gulf of Maine and Bay of Fundy were projected to

TABLE 2 Present-day southern range limit (S Limit), total habitat area (Area), and the allocation of that area to physiological thresholds with poor growth (PG). Each species projected future range shift (RS) in degrees (top; T) and kilometres (bottom; B), new total habitat area (top) and change in area (bottom, italicized), and new allocation of the total habitat area to poor growth (top) and change in allocation (bottom, italicized) for RCP2.6 and 8.5 for GFDL-ESM2M (GFDL) and IPSL-CM5A-LR (IPSL) and the average of the two climate models (AVG) by end-century (2100). See figures for temperatures corresponding to physiological thresholds

| | Present-Day | | | Model | Projections | | | | | |
| | | | | | RCP2.6 | | | RCP8.5 | | |
Species	S Limit (°N)	Area (km²)	PG (%)		RS (T°; B km)	Area (km²)	PG (%)	RS (T°; B km)	Area (km²)	PG (%)
A. nodosum	40.43	406,357	0.31[a]	GFDL	0.14	478,926	0.02[a]	0.72	828,737	0.18[a]
					14	*72,569*	*-0.29[a]*	*70*	*422,380*	*-0.13[a]*
				IPSL	0.29	570,997	0.90[a]	3.08	667,233	2.37[a]
					28	*164,640*	*0.59[a]*	*294*	*260,876*	*2.06[a]*
				AVG	**0.22**	**524,962**	**0.46[a]**	**1.90**	**747,985**	**1.28[a]**
					21	*118,605*	*0.15[a]*	*182*	*341,628*	*0.97[a]*
F. vesiculosus	36.86	380,387	2.47[a,b]	GFDL	0.00	382,347	2.56[a,b]	3.99	407,141	0.18[a,b]
					0	*1,960*	*0.09[a,b]*	*399*	*26,754*	*-2.29[a,b]*
				IPSL	0.75	386,022	0.37[a,b]	4.14	428,505	0.18[a,b]
					77	*5,635*	*-2.10[a,b]*	*413*	*48,118*	*-2.29[a,b]*
				AVG	**0.38**	**384,185**	**1.47[a,b]**	**4.07**	**417,823**	**0.18[a,b]**
					39	*3,798*	*-1.01[a,b]*	*406*	*37,436*	*-2.29[a,b]*
C. crispus	40.43	356,916	0.00	GFDL	-0.14	398,860	0.00	0.72	772,975	0.00
					-14	*41,944*	*0.00*	*70*	*416,059*	*0.00*
				IPSL	0.14	426,104	0.00	1.89	468,685	0.00
					14	*69,188*	*0.00*	*182*	*111,769*	*0.00*
				AVG	**0.00**	**412,482**	**0.00**	**1.31**	**620,830**	**0.00**
					0	*55,566*	*0.00*	*126*	*263,914*	*0.00*
C. fragile	32.48	182,329	12.15[a]	GFDL	0.00	189,581	11.68[a]	0.00	195,314	6.75[a]
					0	*7,252*	*-0.47[a]*	*0*	*12,985*	*-5.40[a]*
				IPSL	0.00	197,813	9.59[a]	0.00	161,602	10.61[a]
					0	*15,484*	*-2.56[a]*	*0*	*-20,727*	*-1.54[a]*
				AVG	**0.00**	**193,697**	**10.64[a]**	**0.00**	**178,458**	**8.68[a]**
					0	*11,368*	*-1.52[a]*	*0*	*-3,871*	*-3.47[a]*

(Continues)

TABLE 2 (Continued)

	Present-Day			Projections						
					RCP2.6			RCP8.5		
Species	S Limit (°N)	Area (km²)	PG (%)	Model	RS (T°; B km)	Area (km²)	PG (%)	RS (T°; B km)	Area (km²)	PG (%)
L. digitata	40.43	334,572	5.23[a,b,c]	GFDL	0.00; 0	328,594 / *−5,978*	5.31[a,b,c] / *0.08[a,b,c]*	0.72; 70	265,041 / *−69,531*	25.90[a,b,c] / *20.67[a,b,c]*
				IPSL	0.00; 0	316,540 / *−18,032*	11.70[a,b,c] / *6.47[a,b,c]*	2.78; 266	160,671 / *−173,901*	27.97[a,b,c] / *22.74[a,b,c]*
				AVG	0.00; 0	**322,567** / *−12,005*	**8.51[a,b,c]** / *3.28[a,b,c]*	1.75; 168	**212,856** / *−121,716*	**26.94[a,b,c]** / *21.71[a,b,c]*
S. latissima	39.43	310,758	6.50[a,b,c]	GFDL	0.00; 0	309,925 / *−833*	6.48[a,b,c] / *−0.02[a,b,c]*	1.79; 175	277,291 / *−33,467*	24.86[a,b,c] / *18.36[a,b,c]*
				IPSL	0.35; 35	312,816 / *2,058*	12.11[a,b,c] / *5.61[a,b,c]*	2.08; 203	211,435 / *−99,323*	23.80[a,b,c] / *17.30[a,b,c]*
				AVG	0.18; 18	**311,371** / *613*	**9.30[a,b,c]** / *2.80[a,b,c]*	1.94; 189	**244,363** / *−66,395*	**24.33[a,b,c]** / *17.83[a,b,c]*

[a]Reduced growth. [b]Partial mortality. [c]Complete mortality. Bold values indicate Average values. Italics indicate Change from present-day values.

have smaller increases in SST than surrounding areas, which limited the overall magnitude of northward shifts of the southern (warm) range limits. For *A. nodosum*, an average 182 km northward shift of its southern edge resulted in minimal habitat area corresponding to reduced growth, but an average 84% increase in total habitat area following northward range expansions (Table 2). For kelps, southern edge shifts 168–189 km northward corresponded to increases in areas with growth reductions and complete mortality. Furthermore, limited northward range expansions resulted in a projected total habitat loss of 36% of *L. digitata* and 21% of *S. latissima* habitat by 2,100.

Fucus vesiculosus was projected to experience a southern (warm) edge shift to Long Island Sound (406 km; Figure 5b,c) and *C. crispus* to the Gulf of Maine (126 km; Figure 2b,c) by 2100. Yet neither species were projected to experience a decrease in habitat suitability in Nova Scotia or the Gulf of St. Lawrence or increases in habitat corresponding to growth reductions. Both *F. vesiculosus* and *C. crispus* were projected to have northward range expansions leading to an overall increase of habitat by 10% and 74%, respectively (Table 2). In comparison, *C. fragile* was projected to experience no southern range shift and minimal northward range expansion that corresponded to an overall habitat loss of 2% (Figure 6b,c).

These species-specific range shifts cumulated to a shift in seaweed richness under RCP8.5 (Figure 8b,c). Both IPSL and GFDL projected a hot spot of richness loss (≥50% of species) from Long Island Sound into the southern Gulf of Maine by 2100, and IPSL also projected a second hot spot in eastern Nova Scotia into the Gulf of St. Lawrence. Both climate models projected the Labrador coast to gain seaweed species richness, with increases throughout the Arctic.

4 | DISCUSSION

Climate change will shift the distribution of many marine species, including foundation species or ecosystem engineers who play key roles in providing habitat structure and other ecosystem functions to associated communities as well as services for human well-being (Pecl et al., 2017). Using SDM and PTs, we projected species-specific range shifts of canopy-forming seaweeds which will alter rocky shore communities along NW-Atlantic coasts. This included a shift in dominance from native to invasive species and a transition to opportunistic life histories. The projected response was dependent on the magnitude of carbon emissions and associated warming, with larger range shifts under the business-as-usual (RCP8.5) compared to the strong mitigation scenario (RCP2.6), highlighting the benefits of climate mitigation. We discuss the projected restructuring of the habitat-forming seaweed community and the consequences this will have for the functions and services they provide.

4.1 | Current drivers of seaweed distribution

Our SDMs found summer SST (M-max) to be a more important driver of seaweed distribution on average than winter SST (M-min) confirming some studies (Assis, Araújo et al., 2018a; Martínez et al., 2018),
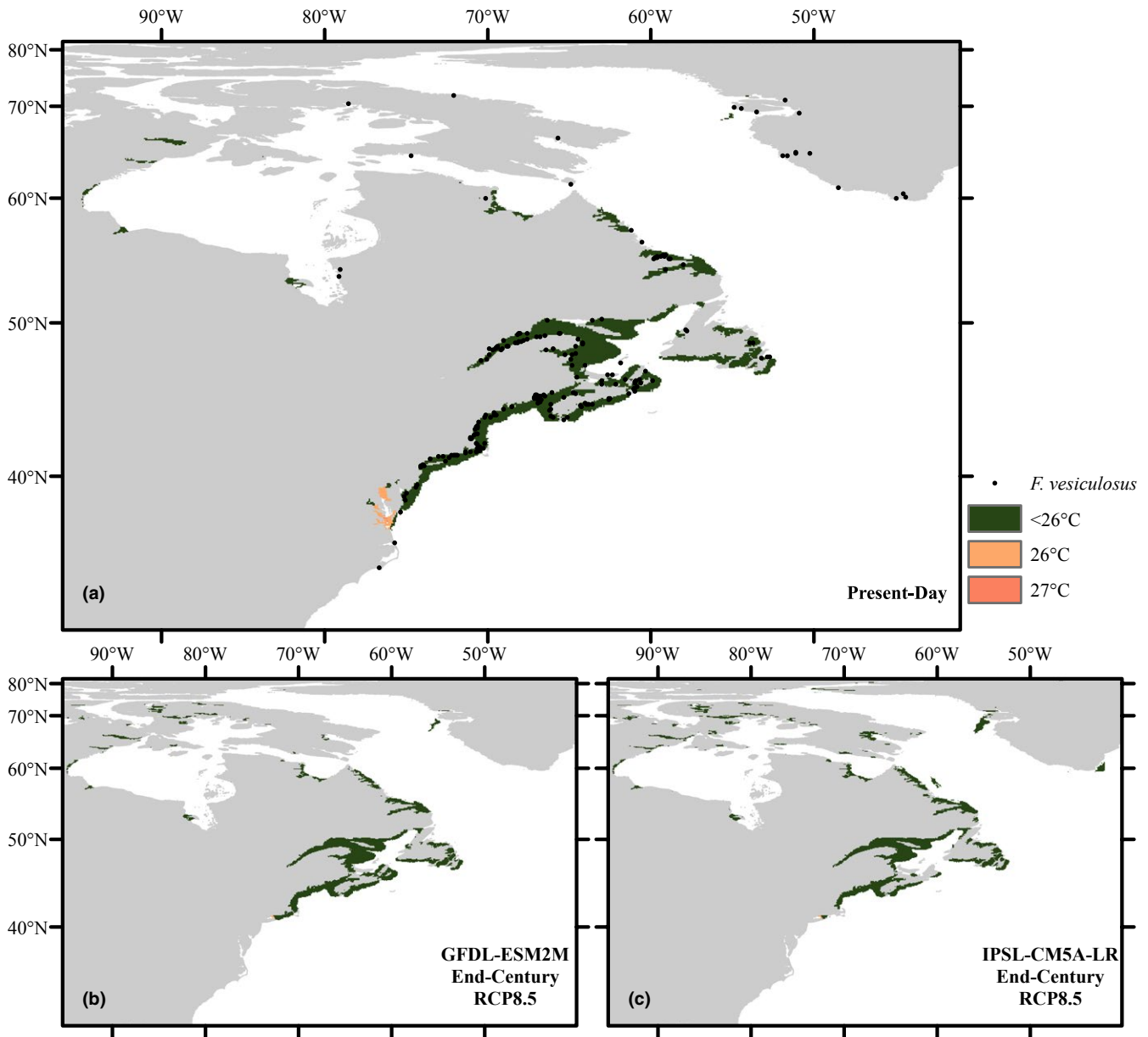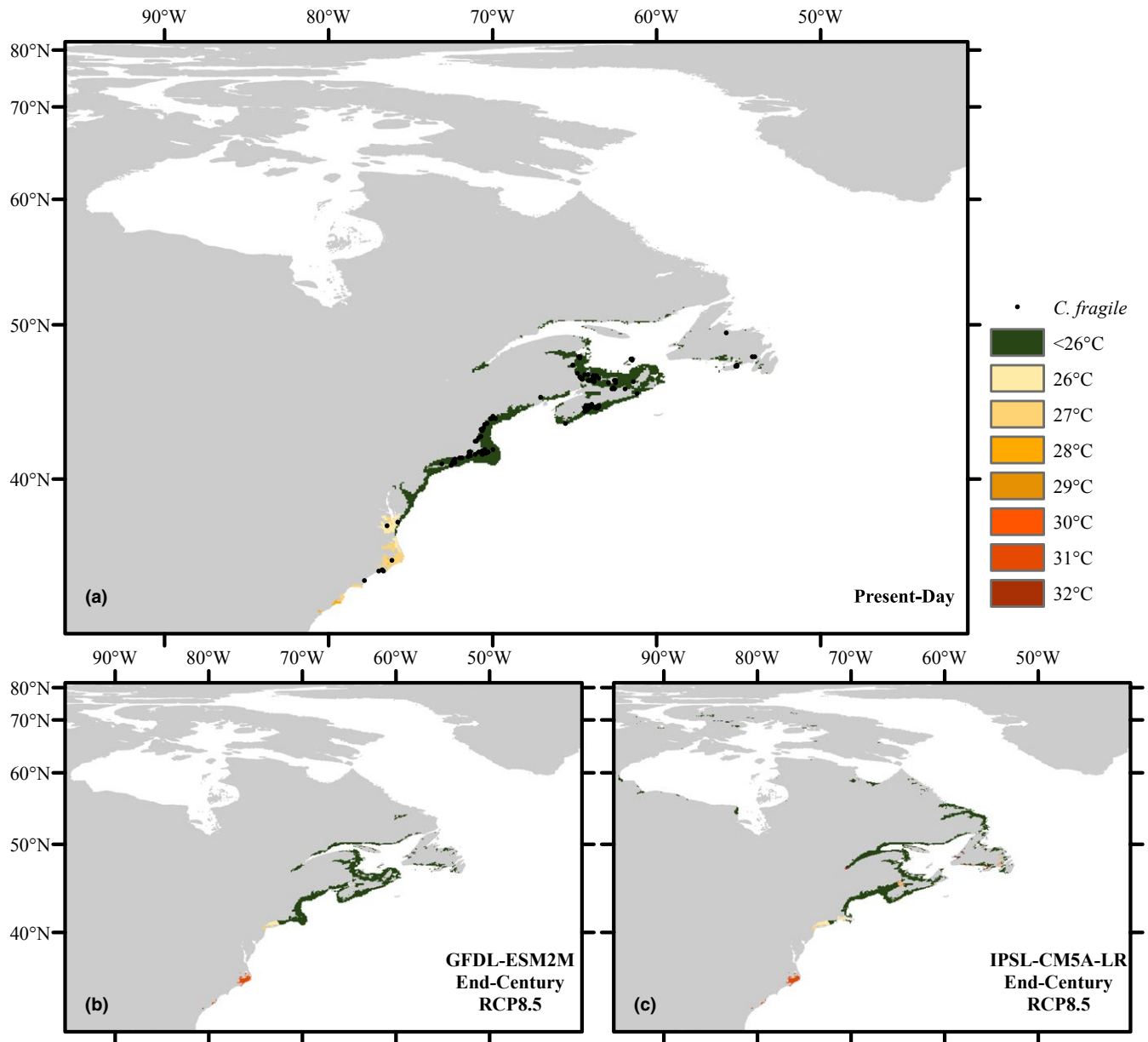
FIGURE 5 Distribution of *Fucus vesiculosus*: (a) present-day occurrence records (black dots) and SDM, and projected (b, c) end-century distribution based on SST changes under RCP8.5 from GFDL-ESM2M (left column) and IPSL-CM5A-LR (right column; Behrmann world equal-area projection). Physiological thresholds were overlaid to show areas of stable growth (green, 12–25°C), and reduced growth and partial mortality (pink-red, 26–28°C); no areas of complete mortality (dark red, ≥29°C). Pixels that appear to be on land are in narrow fjords

while others found the reverse (Franco et al., 2018; Jueterbock et al., 2013). Regardless of season, the dominance of SST as an important predictor was expected as seaweed distributions are primarily defined by SST, and closely follow SST isotherms (Lüning, 1990; van den Hoek, 1975). Increasing summer SST is the primary driver of shifts of the southern (warm) range limit, as SST surpasses growth and mortality thresholds. Whereas, increasing winter SST facilitates faster growth rates (Bolton & Lüning, 1982; Marbà et al., 2017) and greater recruitment (Filbee-Dexter et al., 2016). Diffuse attenuation and sea ice coverage were also important predictors for seaweed distribution. Diffuse attenuation is an indicator of light availability, which sets seaweeds maximum depth limit. Sea ice coverage influences

both the upper vertical distribution limit through ice scour, which often results in bare intertidal zones in the Arctic, and the lower vertical limit by reducing light availability (Krause-Jensen et al., 2012; Küpper et al., 2016). Unlike SST, diffuse attenuation and sea ice coverage are not commonly used as predictor variables; only one study has incorporated diffuse attenuation for fucoids (Jueterbock et al., 2013) and sea ice coverage for kelps (Assis, Araújo et al., 2018a).

As mean SST of the warmest month on average (*M*-max) is an important driver of seaweed distribution and incorporated into each species' SDM, we compared SDM output to warm-temperature PTs to assess the accuracy of our projections. The PTs were based on a standardized laboratory experiment (Wilson et al., 2015) and agreed

FIGURE 6 Distribution of *Codium fragile*: (a) present-day occurrence records (black dots) and SDM, and projected (b, c) end-century distribution based on SST changes under RCP8.5 from GFDL-ESM2M (left column) and IPSL-CM5A-LR (right column; Behrmann world equal-area projection). Physiological thresholds were overlaid to show areas of stable growth (green, 12–25°C), and reduced growth (yellow-dark orange, ≥26°C). Pixels that appear to be on land are in narrow fjords

with model output for fucoids, *C. crispus*, and *C. fragile* but suggested some areas of projected future habitat for kelps corresponding to growth reductions and mortality. Therefore, we may be underestimating the southern edge shift for kelps. Unfortunately, our warm-water PTs cannot provide any information on the species northern range limit; thus, future research could focus on establishing cold-water and light requirement PTs to further refine northern range limits. Other studies have also observed strong agreement between PTs and correlative SDM output (Franco et al., 2018; Martínez et al., 2014). However, neither the SDM nor the PT incorporated the species' potential to acclimate or adapt to increasing SST. Seaweeds are very responsive to acclimatization which can result in greater

tolerance to temperature stress (Harley et al., 2012). Less is known about their ability to adapt to long-term increases in SST, but the occurrence of regional ecotypes suggests it is possible across evolutionary time scales. Yet climate change may occur at rates too fast to allow for adaptive evolution via genetic changes and other adaptation mechanisms may be required (Duarte et al., 2018). For reef-building corals, SDM projected minimal habitat loss by end-century if corals adapted to 1°C warmer SST (Cacciapaglia & van Woesik, 2015), and seaweeds may respond in a similar adaptive manner.

Our projections are based on changes in ocean temperature, which will impact the distribution of intertidal and subtidal species. Yet, air temperature also impacts the distribution of intertidal species
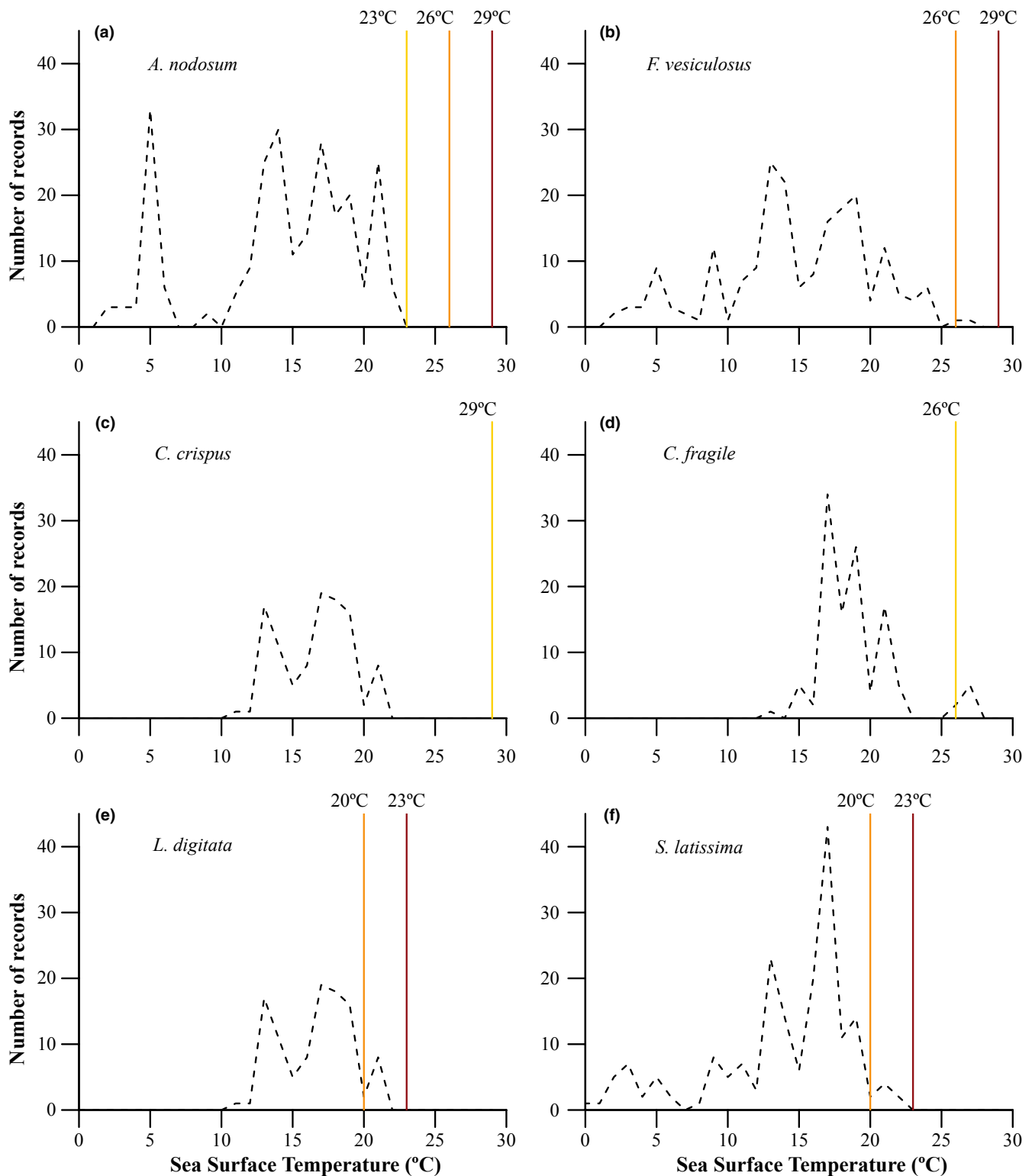
FIGURE 7 Occurrence records plotted against the corresponding sea surface temperature for the warmest month on average (SST *M*-max) for (a) *Ascophyllum nodosum*, (b) *Fucus vesiculosus*, (c) *Chondrus crispus*, (d) *Codium fragile*, (e) *Laminaria digitata* and (f) *Saccharina latissima*. Coloured lines indicate physiological thresholds where yellow is reduced growth, orange is reduced growth and partial mortality, and dark red indicates complete mortality (Wilson et al., 2015)

and under current, observed climate conditions, surface air temperature in the NW-Atlantic is directly correlated with SST in coastal habitats (Loder, Wang, van derBaaren, & Pettipas, 2013). Therefore,

air temperature was not included in our SDM for the intertidal species, but this interaction between surface air temperature and SST may change in a warming climate. Increasing air temperature may
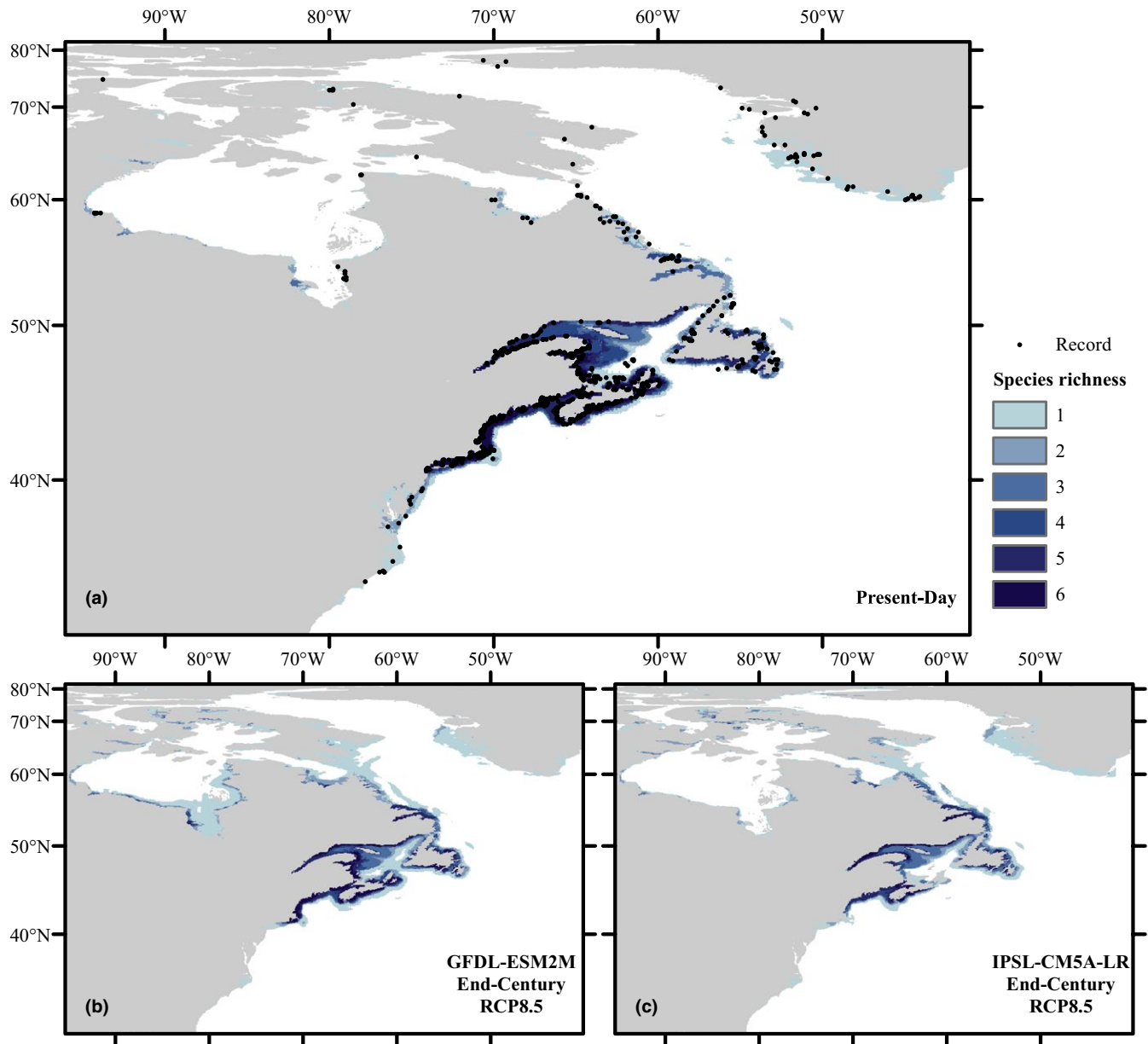
FIGURE 8 Seaweed species richness for (a) present-day occurrence records (black dots) and SDM, and projected (b, c) end-century distribution based on SST changes under RCP8.5 from GFDL-ESM2M (left column) and IPSL-CM5A-LR (right column; Behrmann world equal-area projection)

result in vertical distribution shifts to minimize thermal or desiccation stress during low tide (Harley et al., 2012).

4.2 | Range shifts with climate change

Under the business-as-usual RCP8.5 scenario, we projected species-specific rates of southern (trailing) edge shifts from 0 km per decade for *C. fragile* to 13–19 km per decade for *A. nodosum*, *C. crispus*, and kelps, and 41 km per decade for *F. vesiculosus*, with an average of 18 km per decade. Global meta-analyses of marine species have observed an average trailing edge shift from 15.4 km per decade (Poloczanska et al., 2013) to 19 km per year (Sorte et al., 2010).

Other studies have examined the response of seaweeds to continued SST increases in the NW-Atlantic using different climate models and scenarios. Using older carbon emission scenarios (B1, A1B, A2), Jueterbock et al. (2013) projected an average 3.6° southern range shift for three fucoid species by 2100, and our study projected an average 3.0° southern range shift between *A. nodosum* and *F. vesiculosus* under RCP8.5. Yet, when comparing species-specific responses, our study projected a larger range shift of *A. nodosum* to the Gulf of Maine instead of Delaware Bay (Jueterbock et al., 2013), but a smaller shift of *F. vesiculosus* to Long Island Sound instead of Nova Scotia for A2 (Jueterbock et al., 2013) and RCP8.5 (Assis et al., 2014). Similar to our study, projections for *C. crispus* based on changes in SST isotherms for the B1 scenario also projected a shift

to the Gulf of Maine by 2100 (Müller et al., 2009). B1 projections for *S. latissima* (Müller et al., 2009) and RCP8.5 projections for *S. latissima* and *L. digitata* (Assis, Araújo et al., 2018a) suggested southern range shifts for kelp to Newfoundland, whereas our study projected their existence further south in the northern Gulf of Maine with possible extirpations in parts of Nova Scotia and Gulf of St. Lawrence. No previous study has projected the response of *C. fragile*. Thus, most studies agree on a general northward shift of seaweed distributions, while there is some uncertainty about the magnitude of species-specific shifts. This uncertainty may be driven by the inherent differences and biases between different global climate models and emission scenarios (Bopp et al., 2013). It may also be driven by the intraspecific differences in the responses of NW- and NE-Atlantic populations, which are genetically distinct (Assis et al., 2014; Neiva et al., 2018; Olsen et al., 2010), yet our study trained and projected SDMs within the NW-Atlantic and not the entire North Atlantic as other studies. Lastly, this uncertainty may be due to our calculation of relative changes in SST prior to modelling future projections which had been done for only one of the above-mentioned studies (Müller et al., 2009).

Our SDM projected general expansions of suitable habitat in northern areas for most species; but we do not provide calculations of northern (leading) edge shifts as seaweed occurrence records are very limited in the Arctic. Systematic surveys are either >30 years old (Lee, 1980; Wilce, 1959) or lacking entirely (Filbee-Dexter et al., 2019), although recent surveys have documented seaweed compositions along Baffin Island (Küpper et al., 2016) and Greenland (Høgslund et al., 2014). By incorporating as many northern occurrence records as possible, including older and most up-to-date records, we predicted a much greater northern present-day and projected future distribution for fucoids than previous studies (Assis et al., 2014; Jueterbock et al., 2013). As more detailed Arctic occurrence records become available, our SDM and resulting projections could be further improved to provide higher certainty for species' northern edges.

The projected range expansions in the NW-Atlantic are possible as land masses connect temperate and Arctic seas thereby facilitating dispersal (Krause-Jensen & Duarte, 2014). Northward expansions of seaweeds will depend on each species' dispersal ability, as long-distance dispersal is possible via rafting (Fraser et al., 2018; Kalvas & Kautsky, 1998; Olsen et al., 2010; Trowbridge & Todd, 1999) or kelp zoospores (Reed, Laur, & Ebeling, 1988). It will also depend on the availability of suitable substrate, where rocky coasts are typical along western Greenland and the Canadian Archipelagos but can be limiting elsewhere in the Arctic (Filbee-Dexter et al., 2019). Similar trends are expected for seaweed populations across the Northern Hemisphere in Europe (Assis, Araújo et al., 2018a; Franco et al., 2018; Jueterbock et al., 2013; Raybaud et al., 2013), the Arctic (Jueterbock, Smolina, Coyer, & Hoarau, 2016), and in Japan (Takao, Kumagai, Yamano, Fujii, & Yamanaka, 2015). Yet future studies are needed for the west coast of North America as well as Africa and South America. In the Southern Hemisphere, extinctions are more likely (Martínez et al., 2018) as there are no land masses to promote poleward migration to Antarctica, and strong circumpolar currents limit dispersal abilities, but warming and increased storm events may promote long-distance rafting of kelps (Fraser et al., 2018).

4.3 | Implications for coastal ecosystems

The projected species-specific range shifts, including southern (trailing) edge extinctions, loss of present-day habitat, and expansions of the northern (leading) edge, suggested a restructuring in the composition of canopy-forming seaweeds along rocky shores of the NW-Atlantic, with implications for ecosystem structure, functions and services. Under a business-as-usual RCP8.5 scenario, major changes in seaweed composition are expected from Long Island Sound into the Gulf of Maine, and potentially along the Scotian Shelf and southern Gulf of St. Lawrence, with hot spots for species loss. The loss of canopy-forming species can have cascading effects on coastal ecosystems leading to changes in carbon storage (Schmidt et al., 2011), decreases in secondary production (Krumhansl & Scheibling, 2012), alterations in associated species composition and diversity (Dijkstra et al., 2017; Schmidt & Scheibling, 2006, 2007), and potential regime shifts (Wernberg et al., 2016).

Currently, the Gulf of Maine and Atlantic coast of Nova Scotia are already hot spots for climate change, with greater SST increases than other ocean regions (Pershing et al., 2015) leading to decreases in kelp abundance (Filbee-Dexter et al., 2016; Krumhansl et al., 2016; Witman & Lamb, 2018), shifts in fucoid composition (Ugarte et al., 2010) and commercial fish stock collapses (Pershing et al., 2015). The current commercial rockweed harvest in Gulf of Maine and Canadian Maritimes (Seeley & Schlesinger, 2012) may not be sustained with continued warming as our projections suggest a shift from the dominance of *A. nodosum* with lower tolerance to warmer SST to the more opportunistic *F. vesiculosus* (Wilson et al., 2015). In the subtidal zone of Maine and Nova Scotia, our projections suggested a shift in dominance from native kelp to invasive *C. fragile*, potentially allowing *C. fragile* to settle and form dense beds (Scheibling & Gagnon, 2006). Alternatively, a loss of kelp may facilitate the transition to a turf algae dominated ecosystem (Filbee-Dexter & Wernberg, 2018). To date, the observed warming in the NW-Atlantic has led to increases in both turf-forming and invasive algae in kelp ecosystems (Dijkstra et al., 2017; Filbee-Dexter et al., 2016; Witman & Lamb, 2018), and similar trends have been observed globally (Filbee-Dexter & Wernberg, 2018; Moy & Christie, 2012; Wernberg et al., 2016).

In comparison, projected SST increases, decreases in ice cover, and changing salinity and turbidity patterns in the Arctic will generally have positive effects on the distributional range and production of fucoids and kelps (Filbee-Dexter et al., 2019; Marbà et al., 2017). Yet the projected northward spread of temperate/boreal species may negatively affect established species such as *F. evanescens* (Küpper et al., 2016) and the endemic kelp *L. solidungula* (Filbee-Dexter et al., 2019). Negative interactions following the northward shift of temperate species to polar waters have already resulted in Arctic food web alterations (Kortsch, Primicerio, Fossheim, Dolgov, & Aschan, 2015) and structural changes in fish communities as Arctic species retreat poleward (Fossheim et al., 2015). Lack of baseline data makes

it difficult to quantify if any range shifts, negative or positive interactions have already occurred between temperate and Arctic seaweeds and associated communities. Therefore, detailed studies and ongoing monitoring are needed to understand the consequences of climate change in Arctic ecosystems.

Overall, other habitat-forming species have also been projected to experience poleward range shifts, losses in total suitable habitat area and alteration of species richness patterns. SDM of mangroves projected species-specific poleward latitudinal range shifts of 2°, general losses of total suitable habitat, and shifts in species richness globally (Record et al., 2013). For seagrasses, SDM projected 81.4% of *Zostera noltii*'s current range in the NE-Atlantic to remain as suitable habitat by 2100 with a 888 km northward shift of the range centre (Valle et al., 2014). Furthermore, analysis of carbon sources from coastal sediments in Greenland suggest large increases in seagrass meadows over the 21st century (Marbà, Krause-Jensen, Masqué, & Duarte, 2018). For reef-building corals, SDM projected a loss of 24%–50% of present-day habitat, mainly between 5 and 15° latitudes, poleward expansions, and decreases in coral richness by end-century (Cacciapaglia & van Woesik, 2015). This highlights that many coastal ecosystems around the world will experience shifts in habitat-forming species with ripple effects on dependent communities, including humans.

DATA ACCESSIBILITY

All occurrence records collected are provided in Appendix 1 in Supporting Information. The environmental data are publicly available from the Bio-Oracle dataset (http://www.bio-oracle.org/). All projected climate model data are publicly available from the CMIP5 website (https://cmip.llnl.gov/cmip5/).

ORCID

Kristen L. Wilson https://orcid.org/0000-0002-3685-1531

REFERENCES

Adey, W. H., & Hayek, L.-A.-C. (2011). Elucidating marine biogeography with macrophytes: Quantitative analysis of the North Atlantic supports the thermogeographic model and demonstrates a distinct subarctic region in the Northwestern Atlantic. *Northeastern Naturalist*, *18*, 1–128. https://doi.org/10.1656/045.018.m801

Assis, J., Araújo, M. B., & Serrão, E. A. (2018a). Projected climate changes threaten ancient refugia of kelp forests in the North Atlantic. *Global Change Biology*, *24*, e55–e66. https://doi.org/10.1111/gcb.13818

Assis, J., Serrão, E. A., Claro, B., Perrin, C., & Pearson, G. A. (2014). Climate-driven range shifts explain the distribution of extant gene pools and predict future loss of unique lineages in a marine brown alga. *Molecular Ecology*, *23*, 2797–2810. https://doi.org/10.1111/mec.12772

Assis, J., Tyberghein, L., Bosch, S., Verbruggen, H., Serrão, E. A., & De Clerck, O. (2018b). Bio-ORACLE v2.0: Extending marine data layers for bioclimatic modelling. *Global Ecology and Biogeography*, *27*, 277–284. https://doi.org/10.1111/geb.12693

Barnett, T. P., Pierce, D. W., & Schnur, R. (2001). Detection of anthropogenic climate change in the world's oceans. *Science*, *292*, 270–274. https://doi.org/10.1126/science.1058304

Barry, J. P., Baxter, C. H., Sagarin, R. D., & Gilman, S. E. (1995). Climate-related, long-term faunal changes in a California rocky intertidal community. *Science*, *267*, 672–675. https://doi.org/10.1126/science.267.5198.672

Baumann, H., & Doherty, O. (2013). Decadal changes in the world's coastal latitudinal temperature gradients. *PLoS ONE*, *8*, e67596. https://doi.org/10.1371/journal.pone.0067596

Bolton, J. J., & Lüning, K. (1982). Optimal growth and maximal survival temperatures of Atlantic *Laminaria* species (Phaeophyta) in culture. *Marine Biology*, *66*, 89–94. https://doi.org/10.1007/BF00397259

Bopp, L., Resplandy, L., Orr, J. C., Doney, S. C., Dunne, J. P., Gehlen, M., … Vichi, M. (2013). Multiple stressors of ocean ecosystems in the 21st century: Projections with CMIP5 models. *Biogeosciences*, *10*, 6225–6245. https://doi.org/10.5194/bg-10-6225-2013

Bosch, S., Tyberghein, L., & De Clerck, O. (2018). "sdmpredictors": Species distribution modelling predictor datasets. R Package Version 0.2.6. Retrieved from https://cran.r-project.org/

Cacciapaglia, C., & van Woesik, R. (2015). Reef-coral refugia in a rapidly changing ocean. *Global Change Biology*, *21*, 2272–2282. https://doi.org/10.1111/gcb.12851

Carlton, J. T., & Scanlon, J. (1985). Progression and dispersal of an introduced alga: *Codium fragile* ssp. *tomentosoides* (Chlorophyta) on the Atlantic coast of North America. *Botanica Marina*, *28*, 155–165. https://doi.org/10.1515/botm.1985.28.4.155

Carpenter, K. E., Abrar, M., Aeby, G., Aronson, R. B., Banks, S., Bruckner, A., … Wood, E. (2008). One-third of reef-building corals face elevated extinction risk from climate change and local impacts. *Science*, *321*, 560–563. https://doi.org/10.1126/science.1159196

Chen, I. C., Hill, J. K., Ohlemuller, R., Roy, D. B., & Thomas, C. D. (2011). Rapid range shifts of species associated with high levels of climate warming. *Science*, *333*, 1024–1026. https://doi.org/10.1126/science.1206432

Core Team, R. (2014). *R: A language and environment for statistical computing*. Vienna, Austria: R Foundation for Statistical Computing. Retrieved from http://www.r-project.org/

Dijkstra, J. A., Harris, L. G., Mello, K., Litterer, A., Wells, C., & Ware, C. (2017). Invasive seaweeds transform habitat structure and increase

biodiversity of associated species. *Journal of Ecology*, 105, 1668–1678. https://doi.org/10.1111/1365-2745.12775

Duarte, B., Martins, I., Rosa, R., Matos, A. R., Roleda, M. Y., Reusch, T. B. H., … Jueterbock, A. (2018). Climate change impacts on seagrass meadows and macroalgal forests: An integrative perspective on acclimation and adaptation potential. *Frontiers in Marine Science*, 5, 190. https://doi.org/10.3389/fmars.2018.00190

Duarte, L., Viejo, R. M., Martínez, B., deCastro, M., Gómez-Gesteira, M., & Gallardo, T. (2013). Recent and historical range shifts of two canopy-forming seaweeds in North Spain and the link with trends in sea surface temperature. *Acta Oecologica*, 51, 1–10. https://doi.org/10.1016/j.actao.2013.05.002

Dufresne, J. L., Foujols, M. A., Denvil, S., Caubel, A., Marti, O., Aumont, O., … Vuichard, N. (2013). Climate change projections using the IPSL-CM5 Earth System Model: From CMIP3 to CMIP5. *Climate Dynamics*, 40, 2123–2165. https://doi.org/10.1007/s00382-012-1636-1

Dunne, J. P., John, J. G., Adcroft, A. J., Griffies, S. M., Hallberg, R. W., Shevliakova, E., … Milly, P. (2012). GFDL's ESM2 global coupled climate-carbon earth system models. Part I: Physical formulation and baseline simulation characteristics. *Journal of Climate*, 25, 6646–6665. https://doi.org/10.1175/JCLI-D-11-00560.1

Elith, J., Kearney, M. R., & Phillips, S. J. (2010). The art of modelling range-shifting species. *Methods in Ecology and Evolution*, 1, 330–342. https://doi.org/10.1111/j.2041-210X.2010.00036.x

Elith, J., Phillips, S. J., Hastie, T., Dudík, M., Chee, Y. E., & Yates, C. J. (2011). A statistical explanation of MaxEnt for ecologists. *Diversity and Distributions*, 17, 43–57. https://doi.org/10.1111/j.1472-4642.2010.00725.x

Elith, J., Graham, C. H., Anderson, R. P., Dudik, M., Ferrier, S., Guisan, A., … Zimmermann, N. E. (2006). Novel methods improve prediction of species' distributions from occurrence data. *Ecography*, 29, 129–151. https://doi.org/10.1111/j.2006.0906-7590.04596.x

ESRI (2011). *ArcGIS Desktop: Release 10*. Redlands, CA: Environmental Systems Research Institute.

Field, C., Behrenfeld, M., Randerson, J., & Falkowski, P. (1998). Primary production of the biosphere: Integrating terrestrial and oceanic components. *Science*, 281, 237–240. https://doi.org/10.1126/science.281.5374.237

Filbee-Dexter, K., Feehan, C. J., & Scheibling, R. E. (2016). Large-scale degradation of a kelp ecosystem in an ocean warming hotspot. *Marine Ecology Progress Series*, 543, 141–152. https://doi.org/10.3354/meps11554

Filbee-Dexter, K., & Wernberg, T. (2018). Rise of turfs: A new battlefront for globally declining kelp forests. *Bio-Science*, 68, 64–76. https://doi.org/10.1093/biosci/bix147

Filbee-Dexter, K., Wernberg, T., Fredriksen, S., Norderhaug, K. M., & Pedersen, M. F. (2019). Arctic kelp forests: Diversity, resilience and future. *Global and Planetary Change*, 172, 1–14. https://doi.org/10.1016/j.gloplacha.2018.09.005

Fossheim, M., Primicerio, R., Johannesen, E., Ingvaldsen, R. B., Aschan, M. M., & Dolgov, A. V. (2015). Recent warming leads to a rapid borealization of fish communities in the Arctic. *Nature Climate Change*, 5, 673–677. https://doi.org/10.1038/nclimate2647

Franco, J. N., Tuya, F., Bertocci, I., Rodríguez, L., Martínez, B., Sousa-Pinto, I., & Arenas, F. (2018). The 'golden kelp' *Laminaria ochroleuca* under global change: Integrating multiple eco-physiological responses with species distribution models. *Journal of Ecology*, 106, 47–58. https://doi.org/10.1111/1365-2745.12810

Fraser, C. I., Morrison, A. K., Hogg, A. M. C., Macaya, E. C., van Sebille, E., Ryan, P. G., … Waters, J. M. (2018). Antarctica's ecological isolation will be broken by storm-driven dispersal and warming. *Nature Climate Change*, 8, 704–708. https://doi.org/10.1038/s41558-018-0209-7

Gallon, R. K., Robuchon, M., Leroy, B., Le Gall, L., Valero, M., & Feunteun, E. (2014). Twenty years of observed and predicted changes in subtidal red seaweed assemblages along a biogeographical transition zone: Inferring potential causes from environmental data. *Journal of Biogeography*, 41, 2293–2306. https://doi.org/10.1111/jbi.12380

Hansen, J., Sato, M., Ruedy, R., Lo, K., Lea, D. W., & Medina-Elizade, M. (2006). Global temperature change. *Proceedings of the National Academy of Sciences of the United States of America*, 103, 14288–14293. https://doi.org/10.1073/pnas.0606291103

Harley, C. D. G., Anderson, K. M., Demes, K. W., Jorve, J. P., Kordas, R. L., Coyle, T. A., & Graham, M. H. (2012). Effects of climate change on global seaweed communities. *Journal of Phycology*, 48, 1064–1078. https://doi.org/10.1111/j.1529-8817.2012.01224.x

Hickling, R., Roy, D. B., Hill, J. K., Fox, R., & Thomas, C. D. (2006). The distributions of a wide range of taxonomic groups are expanding polewards. *Global Change Biology*, 12, 450–455. https://doi.org/10.1111/j.1365-2486.2006.01116.x

Hiddink, J. G., & ter Hofstede, R. (2008). Climate induced increases in species richness of marine fishes. *Global Change Biology*, 14, 453–460. https://doi.org/10.1111/j.1365-2486.2007.01518.x

Hijmans, R. J., Phillips, S. J., Leathwick, J. R., & Elith, J. (2017). *"dismo": Species distribution modeling*. R Package Version 1.1-4. Retrieved from https://cran.r-project.org

Høgslund, S., Sejr, M. K., Wiktor, J., Blicher, M. E., & Wegeberg, S. (2014). Intertidal community composition along rocky shores in Southwest Greenland: A quantitative approach. *Polar Biology*, 37, 1549–1561. https://doi.org/10.1007/s00300-014-1541-7

Hutchinson, G. (1957). Concluding remarks. *Cold Spring Harbor Smposia on Quantitative Biology*, 22, 415–427. https://doi.org/10.1101/SQB.1957.022.01.039

IPCC (2013). *Climate change 2013: The physical science basis. Contribution of working group I to the fifth assessment report of the Intergovernmental Panel on Climate Change*. Cambridge, UK: Cambridge University Press.

Jones, C. G., Lawton, J. H., & Shachak, M. (1994). Organisms as ecosystem engineers. *Oikos*, 69, 373–386. https://doi.org/10.2307/3545850

Jueterbock, A., Smolina, I., Coyer, J. A., & Hoarau, G. (2016). The fate of the Arctic seaweed *Fucus distichus* under climate change: An ecological niche modelling approach. *Ecology and Evolution*, 6, 1712–1724. https://doi.org/10.1002/ece3.2001

Jueterbock, A., Tyberghein, L., Verbruggen, H., Coyer, J. A., Olsen, J. L., & Hoarau, G. (2013). Climate change impact on seaweed meadow distribution in the North Atlantic rocky intertidal. *Ecology and Evolution*, 3, 1356–1373. https://doi.org/10.1002/ece3.541

Kalvas, A., & Kautsky, L. (1998). Morphological variation in *Fucus vesiculosus* populations along temperature and salinity gradients in Iceland. *Journal of the Marine Biological Association of the United Kingdom*, 78, 985–1001. https://doi.org/10.1017/S0025315400044921

Kay, L. M., Schmidt, A. L., Wilson, K. L., & Lotze, H. K. (2016). Interactive effects of increasing temperature and nutrient loading on the habitat-forming rockweed *Ascophyllum nodosum*. *Aquatic Botany*, 133, 70–78. https://doi.org/10.1016/j.aquabot.2016.06.002

Keser, M., Swenarton, J. T., & Foertch, J. F. (2005). Effects of thermal input and climate change on growth of *Ascophyllum nodosum* (Fucales, Phaeophyceae) in eastern Long Island Sound (USA). *Journal of Sea Research*, 54, 211–220. https://doi.org/10.1016/j.seares.2005.05.001

Kohavi, R. (1995). A study of cross-validation and bootstrap for accuracy estimation and model selection. *International Joint Conference on Artificial Intelligence*, 14, 1137–1143.

Kortsch, S., Primicerio, R., Fossheim, M., Dolgov, A. V., & Aschan, M. (2015). Climate change alters the structure of arctic marine food webs due to poleward shifts of boreal generalists. *Proceedings of the Royal Society B: Biological Sciences*, 282, 20151546. https://doi.org/10.1098/rspb.2015.1546

Krause-Jensen, D., & Duarte, C. M. (2014). Expansion of vegetated coastal ecosystems in the future Arctic. *Frontiers in Marine Science*, 1, 1–10. https://doi.org/10.3389/fmars.2014.00077

Krause-Jensen, D., Marbà, N., Olesen, B., Sejr, M. K., Christensen, P. B., Rodrigues, J., ... Rysgaard, S. (2012). Seasonal sea ice cover as principal driver of spatial and temporal variation in depth extension and annual production of kelp in Greenland. *Global Change Biology*, *18*, 2981–2994. https://doi.org/10.1111/j.1365-2486.2012.02765.x

Krumhansl, K. A., & Scheibling, R. E. (2012). Detrital subsidy from subtidal kelp beds is altered by the invasive green alga *Codium fragile* ssp. *fragile*. *Marine Ecology Progress Series*, *456*, 73–85. https://doi.org/10.3354/meps09671

Krumhansl, K. A., Okamoto, D. K., Rassweiler, A., Novak, M., Bolton, J. J., Cavanaugh, K. C., ... Byrnes, J. E. K. (2016). Global patterns of kelp forest change over the past half-century. *Proceedings of the National Academy of Sciences of the United States of America*, *113*, 13785–13790. https://doi.org/10.1073/pnas.1606102113

Küpper, F. C., Peters, A. F., Shewring, D. M., Sayer, M. D. J., Mystikou, A., Brown, H., ... Wilce, R. T. (2016). Arctic marine phytobenthos of northern Baffin Island. *Journal of Phycology*, *52*, 532–549. https://doi.org/10.1111/jpy.12417

Lee, R. K. S. (1980). *A catalogue of the marine algae of the Canadian Arctic*. Ottawa, ON, Canada: National Museum of Natural Sciences.

Lima, F. P., Ribeiro, P. A., Queiroz, N., Hawkins, S. J., & Santos, A. M. (2007). Do distributional shifts of northern and southern species of algae match the warming pattern? *Global Change Biology*, *13*, 2592–2604. https://doi.org/10.1111/j.1365-2486.2007.01451.x

Liu, C., Newell, G., & White, M. (2016). On the selection of thresholds for predicting species occurrence with presence-only data. *Ecology and Evolution*, *6*, 337–348. https://doi.org/10.1002/ece3.1878

Loder, J. W., Wang, Z., van derBaaren, A., & Pettipas, R. (2013). Trends and variability of sea surface temperature in the Northwest Atlantic from the HadISST1, ERSST and COBE datasets. *Canadian Technical Report of Hydrography and Ocean Sciences*, *292*, viii + 36p.

Lüning, K. (1990). *Seaweeds their environment, biogeography, and ecophysiology*. New York, NY: John Wiley & Sons Inc.

Marbà, N., Krause-Jensen, D., Masqué, P., & Duarte, C. M. (2018). Expanding Greenland seagrass meadows contribute new sediment carbon sinks. *Scientific Reports*, *8*, 14024. https://doi.org/10.1038/s41598-018-32249-w

Marbà, N., Krause-Jensen, D., Olesen, B., Christensen, P. B., Merzouk, A., Rodrigues, J., ... Wilce, R. T. (2017). Climate change stimulates the growth of the intertidal macroalgae *Ascophyllum nodosum* near the northern distribution limit. *Ambio*, *46*, S119–S131. https://doi.org/10.1007/s13280-016-0873-7

Marcelino, V. R., & Verbruggen, H. (2015). Ecological niche models of invasive seaweeds. *Journal of Phycology*, *51*, 606–620. https://doi.org/10.1111/jpy.12322

Martínez, B., Arenas, F., Trilla, A., Viejo, R. M., & Carreño, F. (2014). Combining physiological threshold knowledge to species distribution models is key to improving forecasts of the future niche for macroalgae. *Global Change Biology*, *21*, 1422–1433. https://doi.org/10.1111/gcb.12655

Martínez, B., Radford, B., Thomsen, M. S., Connell, S. D., Carreño, F., Bradshaw, C. J. A., ... Wernberg, T. (2018). Distribution models predict large contractions of habitat-forming seaweeds in response to ocean warming. *Diversity and Distributions*, *24*, 1350–1366. https://doi.org/10.1111/ddi.12767

Matheson, K., Mckenzie, C. H., Sargent, P., Hurley, M., & Wells, T. (2014). Northward expansion of the invasive green algae *Codium fragile* spp. *fragile* (Suringar) Hariot, 1889 into coastal waters of Newfoundland, Canada. *BioInvasions Records*, *3*, 151–158. https://doi.org/10.3391/bir.2014.3.3.03

Mathieson, A. C., Moore, G. E., & Short, F. T. (2010). A floristic comparison of seaweeds from James Bay and three contiguous Northeastern Canadian arctic sites. *Rhodora*, *119*, 396–434. https://doi.org/10.3119/09-12.1

McDevit, D. C., & Saunders, G. W. (2010). A DNA barcode examination of the Laminariaceae (Phaeophyceae) in Canada reveals novel biogeographical and evolutionary insights. *Phycologia*, *49*, 235–248. https://doi.org/10.2216/PH09-36.1

Merzouk, A., & Johnson, L. E. (2011). Kelp distribution in the Northwest Atlantic Ocean under a changing climate. *Journal of Experimental Marine Biology and Ecology*, *400*, 90–98. https://doi.org/10.1016/j.jembe.2011.02.020

Moss, R. H., Edmonds, J. A., Hibbard, K. A., Manning, M. R., Rose, S. K., van Vuuren, D. P., ... Wilbanks, T. J. (2010). The next generation of scenarios for climate change research and assessment. *Nature*, *463*, 747–756. https://doi.org/10.1038/nature08823

Moy, F. E., & Christie, H. (2012). Large-scale shift from sugar kelp (*Saccharina latissima*) to ephemeral algae along the south and west coast of Norway. *Marine Biology Research*, *8*, 309–321. https://doi.org/10.1080/17451000.2011.637561

Müller, R., Laepple, T., Bartsch, I., & Wiencke, C. (2009). Impact of oceanic warming on the distribution of seaweeds in polar and cold-temperate waters. *Botanica Marina*, *52*, 617–638. https://doi.org/10.1515/BOT.2009.080

Naimi, B., & Araújo, M. B. (2016). SDM: A reproducible and extensible R platform for species distribution modelling. *Ecography*, *39*, 368–375. https://doi.org/10.1111/ecog.01881

Neiva, J., Paulino, C., Nielsen, M. M., Krause-Jensen, D., Saunders, G. W., Assis, J., ... Serrão, E. A. (2018). Glacial vicariance drives phylogeographic diversification in the amphi-boreal kelp *Saccharina latissima*. *Scientific Reports*, *8*, 1112. https://doi.org/10.1038/s41598-018-19620-7

Olsen, J. L., Zechman, F. W., Hoarau, G., Coyer, J. A., Stam, W. T., Valero, M., & Åberg, P. (2010). The phylogeographic architecture of the fucoid seaweed *Ascophyllum nodosum*: An intertidal "marine tree" and survivor of more than one glacial-interglacial cycle. *Journal of Biogeography*, *37*, 842–856. https://doi.org/10.1111/j.1365-2699.2009.02262.x

Parmesan, C., & Yohe, G. (2003). A globally coherent fingerprint of climate change impacts across natural systems. *Nature*, *421*, 37–42. https://doi.org/10.1038/nature01286

Pecl, G. T., Araújo, M. B., Bell, J. D., Blanchard, J., Bonebrake, T. C., Chen, I.-C., ... Williams, S. E. (2017). Biodiversity redistribution under climate change: Impacts on ecosystems and human well-being. *Science*, *355*, eaai9214. https://doi.org/10.1126/science.aai9214

Pereira, H. M., Leadley, P. W., Proenca, V., Alkemade, R., Scharlemann, J. P. W., Fernandez-Manjarres, J. F., ... Walpole, M. (2010). Scenarios for global biodiversity in the 21st century. *Science*, *330*, 1496–1501. https://doi.org/10.1126/science.1196624

Pershing, A. J., Alexander, M. A., Hernandez, C. M., Kerr, L. A., Le Bris, A., Mills, K. E., ... Thomas, A. C. (2015). Slow adaptation in the face of rapid warming leads to collapse of the Gulf of Maine cod fishery. *Science*, *350*, 809–812. https://doi.org/10.1126/science.aac9819

Phillips, S. J., Anderson, R. P., & Schapire, R. E. (2006). Maximum entropy modeling of species geographic distributions. *Ecological Modelling*, *190*, 231–259. https://doi.org/10.1016/j.ecolmodel.2005.03.026

Phillips, S. J., Dudík, M., & Schapire, R. E. (2004). A maximum entropy approach to species distribution modeling. *Proceedings of the Twenty-First Intenational Conference on Machine Learning*, *21*, 655–662. https://doi.org/10.1145/1015330.1015412

Piñeiro-Corbeira, C., Barreiro, R., & Cremades, J. (2016). Decadal changes in the distribution of common intertidal seaweeds in Galicia (NW Iberia). *Marine Environmental Research*, *113*, 106–115. https://doi.org/10.1016/j.marenvres.2015.11.012

Piñeiro-Corbeira, C., Barreiro, R., Cremades, J., & Arenas, F. (2018). Seaweed assemblages under a climate change scenario: Functional responses to temperature of eight intertidal seaweeds match recent abundance shifts. *Scientific Reports*, *8*, 12978. https://doi.org/10.1038/s41598-018-31357-x

Polidoro, B. A., Carpenter, K. E., Collins, L., Duke, N. C., Ellison, A. M., Ellison, J. C., ... Yong, J. W. H. (2010). The loss of species: Mangrove

extinction risk and geographic areas of global concern. *PLoS ONE, 5,* e10095. https://doi.org/10.1371/journal.pone.0010095

Poloczanska, E. S., Brown, C. J., Sydeman, W. J., Kiessling, W., Schoeman, D. S., Moore, P. J., ... Richardson, A. J. (2013). Global imprint of climate change on marine life. *Nature Climate Change, 3,* 919–925. https://doi.org/10.1038/nclimate1958

Provan, J., Booth, D., Todd, N. P., Beatty, G. E., & Maggs, C. A. (2008). Tracking biological invasions in space and time: Elucidating the invasive history of the green alga *Codium fragile* using old DNA. *Diversity and Distributions, 14,* 343–354. https://doi.org/10.1111/j.1472-4642.2007.00420.x

Raybaud, V., Beaugrand, G., Goberville, E., Delebecq, G., Destombe, C., Valero, M., ... Gevaert, F. (2013). Decline in kelp in West Europe and climate. *PLoS ONE, 8,* e66044. https://doi.org/10.1371/journal.pone.0066044

Record, S., Charney, N. D., Zakaria, R. M., & Ellison, A. M. (2013). Projecting global mangrove species and community distributions under climate change. *Ecosphere, 4,* 34. https://doi.org/10.1890/ES12-00296.1

Redmond, S. (2013). *Effects of increasing temperature and ocean acidification on the microstages of two populations of* Saccharina latissima *in the Northwest Atlantic*. MSc thesis, University of Connecticut, vi + 51.

Reed, D. C., Laur, D. R., & Ebeling, A. W. (1988). Variation in algal dispersal and recruitment: The importance of episodic events. *Ecological Monographs, 58,* 321–335. https://doi.org/10.2307/1942543

Scheibling, R. E., & Gagnon, P. (2006). Competitive interactions between the invasive green alga *Codium fragile* ssp. *tomentosoides* and native canopy-forming seaweeds in Nova Scotia (Canada). *Marine Ecology Progress Series, 325,* 1–14. https://doi.org/10.3354/meps325001

Schmidt, A. L., Coll, M., Romanuk, T. N., & Lotze, H. K. (2011). Ecosystem structure and services in eelgrass *Zostera marina* and rockweed *Ascophyllum nodosum* habitats. *Marine Ecology Progress Series, 437,* 51–68. https://doi.org/10.3354/meps09276

Schmidt, A. L., & Scheibling, R. E. (2006). A comparison of epifauna and epiphytes on native kelps (*Laminaria* species) and an invasive alga (*Codium fragile* ssp. *tomentosoides*) in Nova Scotia, Canada. *Botanica Marina, 49,* 315–330. https://doi.org/10.1515/BOT.2006.039

Schmidt, A. L., & Scheibling, R. E. (2007). Effects of native and invasive macroalgal canopies on composition and abundance of mobile benthic macrofauna and turf-forming algae. *Journal of Experimental Marine Biology and Ecology, 341,* 110–130. https://doi.org/10.1016/j.jembe.2006.10.003

Seeley, R. H., & Schlesinger, W. H. (2012). Sustainable seaweed cutting? The rockweed (*Ascophyllum nodosum*) industry of Maine and the Maritime Provinces. *Annals of the New York Academy of Sciences, 1249,* 84–103. https://doi.org/10.1111/j.1749-6632.2012.06443.x

Short, F. T., Polidoro, B. A., Livingstone, S. R., Carpenter, K. E., Bandeira, S., Bujang, J. S., ... Zieman, J. C. (2011). Extinction risk assessment of the world's seagrass species. *Biological Conservation, 144,* 1961–1971. https://doi.org/10.1016/j.biocon.2011.04.010

Simonson, E., Scheibling, R. E., & Metaxas, A. (2015). Kelp in hot water: I. Warming seawater temperature induces weakening and loss of kelp tissue. *Marine Ecology Progress Series, 537,* 89–104. https://doi.org/10.3354/meps11438

Sorte, C. J. B., Williams, S. L., & Carlton, J. T. (2010). Marine range shifts and species introductions: Comparative spread rates and community impacts. *Global Ecology and Biogeography, 19,* 303–316. https://doi.org/10.1111/j.1466-8238.2009.00519.x

Sunday, J. M., Bates, A. E., & Dulvy, N. K. (2012). Thermal tolerance and the global redistribution of animals. *Nature Climate Change, 2,* 686–690. https://doi.org/10.1038/nclimate1539

Takao, S., Kumagai, N. H., Yamano, H., Fujii, M., & Yamanaka, Y. (2015). Projecting the impacts of rising seawater temperatures on the distribution of seaweeds around Japan under multiple climate change scenarios. *Ecology and Evolution, 5,* 213–223. https://doi.org/10.1002/ece3.1358

Talluto, M. V., Boulangeat, I., Ameztegui, A., Aubin, I., Berteaux, D., Butler, A., ... Gravel, D. (2016). Cross-scale integration of knowledge for predicting species ranges: A metamodelling framework. *Global Ecology and Biogeography, 25,* 238–249. https://doi.org/10.1111/geb.12395

Tanaka, K., Taino, S., Haraguchi, H., Prendergast, G., & Hiraoka, M. (2012). Warming off southwestern Japan linked to distributional shifts of subtidal canopy-forming seaweeds. *Ecology and Evolution, 2,* 2854–2865. https://doi.org/10.1002/ece3.391

Taylor, K. E., Stouffer, R. J., & Meehl, G. A. (2012). An overview of CMIP5 and the experiment design. *Bulletin of the American Meteorological Society, 93,* 485–498. https://doi.org/10.1175/BAMS-D-11-00094.1

Taylor, W. R. (1957). *Marine algae of the northeastern coast of North America* (2nd ed.). Ann Arbor, MI: The University of Michigan Press.

Tittensor, D. P., Mora, C., Jetz, W., Lotze, H. K., Ricard, D., Berghe, E. V., & Worm, B. (2010). Global patterns and predictors of marine biodiversity across taxa. *Nature, 466,* 1098–1101. https://doi.org/10.1038/nature09329

Trowbridge, C. D., & Todd, C. D. (1999). The familiar is exotic: I. *Codium fragile* ssp. *atlanticum* on Scottish rocky intertidal shores. *Botanical Journal of Scotland, 51,* 161–179. https://doi.org/10.1080/03746609908684932

Tyberghein, L., Verbruggen, H., Pauly, K., Troupin, C., Mineur, F., & De Clerck, O. (2012). Bio-ORACLE: A global environmental dataset for marine species distribution modelling. *Global Ecology and Biogeography, 21,* 272–281. https://doi.org/10.1111/j.1466-8238.2011.00656.x

Ugarte, R. A., Craigie, J. S., & Critchley, A. T. (2010). Fucoid flora of the rocky intertidal of the Canadian Maritimes: Implications for the future with rapid climate change. In J. Seckbach, R. Einav, & A. Israel (Eds.), *Seaweeds and their role in globally changing environments* (Vol. 15, pp. 69–90). Dordrecht, the Netherlands: Springer Netherlands.

Valle, M., Chust, G., del Campo, A., Wisz, M. S., Olsen, S. M., Garmendia, J. M., & Borja, Á. (2014). Projecting future distribution of the seagrass *Zostera noltii* under global warming and sea level rise. *Biological Conservation, 170,* 74–85. https://doi.org/10.1016/j.biocon.2013.12.017

van den Hoek, C. (1975). Phytogeographic provinces along the coasts of the northern Atlantic Ocean. *Phycologia, 14,* 317–330. https://doi.org/10.2216/i0031-8884-14-4-317.1

Wernberg, T., Russell, B. D., Thomsen, M. S., Gurgel, C. F. D., Bradshaw, C. J. A., Poloczanska, E. S., & Connell, S. D. (2011). Seaweed communities in retreat from ocean warming. *Current Biology, 21,* 1828–1832. https://doi.org/10.1016/j.cub.2011.09.028

Wernberg, T., Bennett, S., Babcock, R. C., Bettignies, T. D., Cure, K., Depczynski, M., ... Wilson, S. (2016). Climate-driven regime shift of a temperate marine ecosystem. *Science, 353,* 169–172. https://doi.org/10.1126/science.aad8745

Wilce, R. T. (1959). *The marine algae of the Labrador Peninsula and Northwest Newfoundland (Ecology and Distribution)*. Ottawa, ON, Canada: National Musuem of Canada.

Wilson, K. L., Kay, L. M., Schmidt, A. L., & Lotze, H. K. (2015). Effects of increasing water temperatures on survival and growth of ecologically and economically important seaweeds in Atlantic Canada: Implications for climate change. *Marine Biology, 162,* 2431–2444. https://doi.org/10.1007/s00227-015-2769-7

Witman, J. D., & Lamb, R. W. (2018). Persistent differences between coastal and offshore kelp forest communities in a warming Gulf of Maine. *PLoS ONE, 13,* e0189388. https://doi.org/10.1371/journal.pone.0189388

Worm, B., & Lotze, H. K. (2006). Effects of eutrophication, grazing, and algal blooms on rocky shores. *Limnology and Oceanography, 51,* 569–579. https://doi.org/10.4319/lo.2006.51.1_part_2.0569

Yesson, C., Bush, L. E., Davies, A. J., Maggs, C. A., & Brodie, J. (2015). Large brown seaweeds of the British Isles: Evidence of changes in abundance over four decades. *Estuarine, Coastal and Shelf Science, 155,* 167–175. https://doi.org/10.1016/j.ecss.2015.01.008

Yost, A. C., Petersen, S. L., Gregg, M., & Miller, R. (2008). Predictive modeling and mapping sage grouse (*Centrocercus urophasianus*) nesting habitat using Maximum Entropy and a long-term dataset from Southern Oregon. *Ecological Informatics*, *3*, 375–386. https://doi.org/10.1016/j.ecoinf.2008.08.004

BIOSKETCHES

Kristen L Wilson is a Research Associate in the Department of Biology at Dalhousie University. Her research examines human impacts on marine macrophytes in coastal ecosystems, using species distribution models and remote sensing.

Marc A. Skinner is Stantec's Consulting Marine Ecosystem Technical Leader, and an Adjunct Professor with the Faculty of Graduate Studies at Dalhousie University. His research focuses on environmental assessments, with a focus on monitoring of marine and freshwater habitats.

Heike K. Lotze is a Professor in the Department of Biology at Dalhousie University. Her research program focuses on human-induced changes in marine ecosystems, including the effects of climate change, habitat alteration, exploitation and pollution, and their consequences for ecosystem structure, functions and services.

Author contributions: KLW, MAS, HKL conceived and designed the framework for the study. KLW compiled and analysed the data and drafted the original manuscript. KLW, MAS, HKL contributed substantially to manuscript writing and review.

SUPPORTING INFORMATION

Additional supporting information may be found online in the Supporting Information section at the end of the article.